Parameter Estimation Based Fault Detection and Isolation in Electrohydraulic Systems

by

Ruixiang SONG

A Thesis
Submitted to the Faculty of Graduate Studies
In Partial Fulfillment of the Requirements
for the Degree of

Master of Science

Department of Mechanical and Industrial Engineering
University of Manitoba
Winnipeg, Manitoba

© May,2002

National Library of Canada
Bibliothèque nationale du Canada

Acquisitions and Bibliographic Services
Acquisitions et services bibliographiques

395 Wellington Street
Ottawa ON K1A 0N4
Canada

395, rue Wellington
Ottawa ON K1A 0N4
Canada

Your file Votre référence

Our file Notre référence

The author has granted a non-exclusive licence allowing the National Library of Canada to reproduce, loan, distribute or sell copies of this thesis in microform, paper or electronic formats.

L'auteur a accordé une licence non exclusive permettant à la Bibliothèque nationale du Canada de reproduire, prêter, distribuer ou vendre des copies de cette thèse sous la forme de microfiche/film, de reproduction sur papier ou sur format électronique.

The author retains ownership of the copyright in this thesis. Neither the thesis nor substantial extracts from it may be printed or otherwise reproduced without the author's permission.

L'auteur conserve la propriété du droit d'auteur qui protège cette thèse. Ni la thèse ni des extraits substantiels de celle-ci ne doivent être imprimés ou autrement reproduits sans son autorisation.

0-612-80031-8

Canada

THE UNIVERSITY OF MANITOBA

FACULTY OF GRADUATE STUDIES

*****

COPYRIGHT PERMISSION

PARAMETER ESTIMATION BASED FAULT DETECTION AND ISOLATION IN ELECTROHYDRAULIC SYSTEMS

BY

RUIXIANG SONG

A Thesis/Practicum submitted to the Faculty of Graduate Studies of The University of Manitoba in partial fulfillment of the requirement of the degree

of

MASTER OF SCIENCE

RUIXIANG SONG © 2002

Permission has been granted to the Library of the University of Manitoba to lend or sell copies of this thesis/practicum, to the National Library of Canada to microfilm this thesis and to lend or sell copies of the film, and to University Microfilms Inc. to publish an abstract of this thesis/practicum.

This reproduction or copy of this thesis has been made available by authority of the copyright owner solely for the purpose of private study and research, and may only be reproduced and copied as permitted by copyright laws or with express written authorization from the copyright owner.

Abstract

In this work, a fault detection and isolation strategy based on parameter estimation, a widely used method in system identification, is employed for a servo-positioning hydraulic system. Model selection criteria for fault detection and isolation purposes are presented and elaborated. The batch least squares method, well known for linear time-invariant system identification, is employed to estimate the coefficients of the selected model. The relationship between the estimated model coefficients and the actual physical parameters is explored empirically. Direct threshold checking is used as the basic fault detection and isolation logic. The performance of this strategy is evaluated based on fault conditions due to incorrect supply pump pressure and changes in equivalent viscous damping coefficient. It is shown that fault detection and isolation for faults due to a change in a single physical parameter can be achieved. However, complete fault detection and isolation is both difficult and conditional for faults originating from changes in more than one physical parameter.

Acknowledgements

Firstly, I wish to thank my advisor, Dr. N. Sepehri for creating a free and comfortable environment for my study and research work at the University of Manitoba. Throughout the course of my project, he provided good suggestions and encouragement, which were full of originality and imagination. I also owe him much for sharing my frustrations during my work.

Secondly, I would like to express my appreciation to Mark Karpenko and Al. Lohse for their great help in developing the simulation program, building the test station and developing the interfacing program.

My good friends, Mr. and Mrs. Trebacz, Liang An, Zonghui Zheng, Bin Ma, Xiuping Mu, and all the people who care for me in Canada, I thank you very much for your friendship and help during this most precious and valuable period of my life.

Finally, and most important of all, I thank my family for their always-true love, devotion and support.

Table of Contents

List of Figures

List of Tables

Chapter 1 Introduction

With the development of our society, engineering systems are becoming more and more functional and complicated. For example, in an airplane, thousands of inter-dependent electrical and mechanical units are integrated. In such a complex system, failure of one unit may cause a loss of millions of dollars and even hundreds of lives. The requirements for fault-tolerance, reliability and security have triggered the demand for thorough maintenance checks and monitoring systems, so as to detect faulty components, and make the systems more robust. Maintenance checks are usually performed on a regular basis off-line by technicians. On the other hand, monitoring systems gather information about the units of the system and make decisions about the working conditions of the monitored system.

1.1 Motivation

Fault detection and isolation strategy is the key component of the monitoring system. Traditional fault detection and isolation systems are based on hardware redundancy and a voting logic. With the rapid development of inexpensive, high-speed computers and digital signal processing (DSP) technologies, functional redundancy (a software approach) based fault detection and isolation systems are becoming increasingly popular [3]. Since the states or the parameters of a monitored process are closer to the process faults in terms of signal flow, observer based state estimation theory [1,2] and on-line system parameter estimation technologies [9] are well developed and employed in fault detection and isolation for linear time-invariant systems. Among those technologies, unknown input observer (UIO) [4] and least squares (LS) parameter estimation [5]

methods can be named. The UIO method provides a robust residual generation in the presence of unknown inputs, disturbances, modeling uncertainties, physical parameter variation and measurement noise. The LS parameter estimation method provides a powerful way of detecting faults by monitoring on line the estimates of the dynamic system's physical parameters. However, for cases where explicit models cannot be derived or for nonlinear dynamic systems, such as hydraulic systems, the application of UIO and LS methods for fault detection and isolation becomes very challenging [4,5].

Hydraulic systems are widely used in machine tool applications and aircraft control systems. Compared with other systems, using hydraulic systems has the following advantages [10]:

1. Hydraulic fluid acts as a lubricant, in addition to carrying away heat generated in the system to a convenient heat exchanger.
2. Comparatively small hydraulic actuators can develop large force or torque.
3. Hydraulic actuators have a higher speed of response with fast starts, stops, and reversals.
4. Hydraulic actuators can operate under continuous, intermittent, reversing and stalled conditions without damage.
5. Availability of both linear and rotary actuators gives flexibility in design.
6. Because of low leakage in hydraulic actuators, speed drop is small when load is applied.

There are, however, several disadvantages in the application of hydraulic systems [10]:

1. Hydraulic power is not readily available as compared to electric power.

2. The cost of a hydraulic system may be higher than a comparable electrical system performing a similar function.
3. Fire and explosion hazards exist.
4. It is difficult to maintain a hydraulic system that is free from leaks. Thus the system tends to be messy.
5. Contaminated oil may cause failure in the proper functioning of a hydraulic system.
6. Hydraulic circuits have generally poor damping characteristics. If a hydraulic circuit is not designed properly, some unstable phenomena may occur depending upon the operating condition.
7. The design of a hydraulic system is quite involved due to nonlinear and other complex characteristics.

Wide application together with nonlinear and complex characteristics make the functional redundancy based fault detection and isolation for hydraulic systems a very attractive field. Faults in hydraulic systems can be grouped into incorrect supply pump pressure, increased internal and external leakage, and changes in hydraulic compliance [13].

1.2 Objective and Scope of This Thesis

Previous work on fault detection and isolation for hydraulic systems has mainly been based on linear, bilinear and nonlinear observer based approaches [15,16]. In this work, a parameter estimation based fault detection and isolation strategy is attempted for a double-rod electrohydraulic actuator. An autoregressive with exogenous input (ARX) model is selected according to model selection criteria and the LS parameter estimation

method is employed to estimate the coefficients of the selected model. Direct threshold checking is then applied as the basic fault detection and isolation logic.

In Chapter 2, a review of fault detection is provided. Two important tools for fault detection and isolation in linear time-invariant systems, i.e., UIO and parametric estimation methods, are specifically discussed in this chapter. Chapter 3 outlines the general procedure for parameter estimation based fault detection and isolation. The nonlinear hydraulic system model is derived for simulation purposes in Chapter 4. Simulation and experimental tests are performed in Chapters 5 and 6, and conclusions are presented in Chapter 7.

Chapter 2 Background Study

In this chapter, the development of fault detection and isolation is reviewed. Traditional hardware redundancy based strategies and functional redundancy based strategies are outlined. Unknown input observer and parametric estimation methods for linear time-invariant systems are presented.

2.1 Hardware Redundancy Based Fault Detection and Isolation

Since sensors provide vital information for controllers within the control system, early monitoring schemes are primarily concerned with the sensor fault detection, also called instrument fault detection (IFD). Traditionally, this type of fault detection is achieved through hardware redundancy. In such a scheme, more than two similar sensors (usually three or four) are used to measure the same variable of the monitored system. A voting logic is adopted in decision making. One sensor is to be declared as faulty when its signal is too far away from the average of signals from other sensors. The monitoring system identifies the faulty sensors and the average of signals from those sensors that are working properly is taken as the true value of the measured variable. Thus, the monitored system can still work properly in the presence of a sensor fault condition. This approach is quite simple, reasonably straightforward and widely used. However, there are several shortcomings to this scheme. The major problems are:

1. Extra hardware and software costs for redundant sensors.
2. Extra physical space required for the installation of extra sensors.
3. Conditions that can cause one sensor to fail may damage redundant sensors as well.

4. Fault conditions other than sensor fault cannot be detected.

2.2 Functional Redundancy Based Fault Detection and Isolation

With the rapid development of inexpensive, powerful and reliable computers, alternative approaches have been attempted to overcome (at least in part) the problems of hardware redundancy based fault detection and isolation and to improve the overall reliability of the monitored system. New approaches have been prompted since the 1970's by the high cost of redundant sensors and the excessive weight and space demands imposed on the system. These approaches are based on the idea of using several dissimilar sensors to measure different variables of the same process, instead of using several similar sensors to measure the same variable of the process. Since the signals from the dissimilar sensors are all driven by the same dynamic process, these approaches are called functional redundancy (also called analytical redundancy or artificial redundancy). The basic idea of functional redundancy to instrument fault detection is the observer (state estimator) theory, which was proposed by Lunenberger in the 1960's [1,2].

Observer based instrument fault detection is very similar to the hardware redundancy based fault detection scheme. For example, there are several sensors measuring different variables of the same process. If observability [10] is satisfied, signal(s) from one or some of these sensors can drive an observer to estimate other signals. The estimated signals from the observer can be used to compare with the actual signals, which are not used to drive the observer. If the sensors whose signals are used to drive the observer are faulty, all the estimated signals will deviate from the actual ones. If only one of the estimated signals is far away from the corresponding actual one, the

sensor for that particular signal is considered faulty. Through designing different observers which are driven by different set of signals, many sensor faults can be detected and isolated.

Along with observer based fault detection theory, parameter estimation, adaptive filtering, variable threshold logic and statistical decision theory can also be implemented within a functional redundancy based fault detection and isolation (FDI) strategy [3]. Normally, both the input signals to and the output signals from the monitored process are required for a functional redundancy based FDI scheme. These schemes are therefore designed under assumptions that [3]:

1. Either the dynamic nature of the system being monitored is precisely known to a reasonable degree.
2. Or it is possible to determine the value of certain physical parameters by on-line identification techniques applied to the input and output signals of the monitored plant.

Since the states or the parameters of the monitored process are closer to the process faults in terms of signal flow, observer based state estimation theories and system parameter estimation technologies are well-developed and used in fault detection and isolation for linear time-invariant (LTI) systems. Among them, unknown input observer (UIO) [4] and least squares (LS) parameter estimation [5] are commonly used. They will be briefly described here.

2.2.1 Fault Diagnosis Based on Unknown Input Observer

One of the challenges in achieving a robust fault detection and isolation scheme is to reach complete de-coupling and hence invariance between different fault effects, or

between the effects of faults and the effects of unknown inputs which are independent of the fault mode. The unknown input observer approach can fulfill this task through transforming the state equations, which represent system dynamics, fault and possible unknown inputs, into a Kronecker Canonical Form (KCF) [4]. Consider the system that is described by the following discrete-time state equations:

$$\boldsymbol{x}_{k+1} = \boldsymbol{A}\boldsymbol{x}_k + \boldsymbol{B}\boldsymbol{u}_k + \boldsymbol{E}\boldsymbol{d}_k + \boldsymbol{K}\boldsymbol{f}_k \tag{2-1}$$

$$\boldsymbol{y}_k = \boldsymbol{C}\boldsymbol{x}_k \tag{2-2}$$

where

$\boldsymbol{x}_k$ $(n \times 1)$ represents the state vector at the sampling instant k.

$\boldsymbol{A}$ $(n \times n)$ is the system matrix.

$\boldsymbol{B}$ $(n \times r)$ represents the known input distribution matrix.

$\boldsymbol{u}_k$ $(r \times 1)$ represents the known input vector at the sampling instant k.

$\boldsymbol{E}$ $(n \times s)$ represents the unknown input distribution matrix.

$\boldsymbol{d}_k$ $(s \times 1)$ represents the unknown input vector at the sampling instant k.

$\boldsymbol{K}$ $(n \times w)$ represents the fault distribution matrix.

$\boldsymbol{f}_k$ $(w \times 1)$ represents the fault vector at the sampling instant k.

$\boldsymbol{C}$ $(m \times n)$ represents the measurement matrix.

$\boldsymbol{y}_k$ $(m \times 1)$ represents the measurement of system output at the sampling instant k.

$\boldsymbol{A}$, $\boldsymbol{B}$, $\boldsymbol{C}$, $\boldsymbol{E}$ and $\boldsymbol{K}$ are required to be perfectly known for the purpose of observer design. An unknown input fault detection observer for the system described by equations (2-1) and (2-2) has the following structure:

$$\boldsymbol{z}_{k+1} = \boldsymbol{F}\boldsymbol{z}_k + \boldsymbol{J}\boldsymbol{u}_k + \boldsymbol{G}\boldsymbol{y}_k \tag{2-3}$$

$$r_k = L_1 z_k + L_2 y_k \tag{2-4}$$

where $z_k\,(t \times 1)$ denotes the state of the observer and $r_k\,(v \times 1)$ is the residual. This observer exists if and only if:

1. For any initial condition x_0 and z_0, if no fault happens, i.e., $f_k = 0$, then $\lim_{k->\infty} r_k = 0$.
2. Given a $(t \times n)$ transforming matrix T, if $z_0 = Tx_0$ and $f_k = 0$, then $z_k = Tx_k$ for all $k \geq 0$.
3. For $z_0 = Tx_0$, if any arbitrary $f_k \neq 0$, then $r_k \neq 0$.

In [4], the necessary and sufficient condition of the existence of this observer is given. With the help of the algorithm presented in [6] and [7], the procedure of deriving matrices F, J, G, L_1 and L_2 is also described.

Although it leads to the most powerful model-based fault detection and isolation approaches for disturbed and uncertain dynamic systems, the limitation of this approach is quite obvious. The exact linear model of the system is required and the distribution of the uncertainty and disturbance must also be understood in detail. For the cases of nonlinear dynamic systems or of poorly precise models of linear systems, this method is cumbersome and the complete isolation between the unknown inputs and the faults is difficult to achieve.

2.2.2 Fault Diagnosis Based on Model Parameter Estimation

Generally, the behavior of a system process is a function of the system's initial condition, input signal and physical parameters and is governed by physical laws. When these physical laws are well understood, this function can be expressed as a set of

ordinary or partial differential equations. The coefficients of the resulting equations are functions of the system's physical parameters [5].

If a system can be described by linear differential equations, the least squares method can be employed to estimate the coefficients of the equations. For example, a discrete linear time-invariant single-input-single-output system can be expressed as in equation (2-5).

$$\begin{aligned} &y(t)+a_1y(t-1)+a_2y(t-2)+\cdots+a_ny(t-n)\\ &=b_1u(t-1)+b_2u(t-2)+\cdots+b_mu(t-m) \end{aligned} \tag{2-5}$$

Equation (2-5) shows that the current output of the system is a linear combination of the past n outputs and past m inputs. It can be written in the following form:

$$y(t)=\boldsymbol{\theta}^T\boldsymbol{\psi}(t) \tag{2-6}$$

where

$$\boldsymbol{\psi}^T(t)=\left[-y(t-1),-y(t-2),\cdots,-y(t-n),u(t-1),\cdots,u(t-m)\right]$$

and

$$\boldsymbol{\theta}^T=[a_1,a_2,\cdots,a_n,b_1,\cdots,b_m]$$

The input and output signals are measured at discrete times $t=kT_s$, $k=1,2,\cdots,N$, where T_s is the sampling period. Suppose $\hat{\boldsymbol{\theta}}$ is the estimation of $\boldsymbol{\theta}$, then

$$e(t)=y(t)-\hat{\boldsymbol{\theta}}^T\boldsymbol{\psi}(t) \tag{2-7}$$

The loss function is defined as

$$J=\sum_{t=1}^{N}\alpha_t e^2(t) \tag{2-8}$$

$$\boldsymbol{e}^T=[e(1),e(2)\cdots,e(N)] \tag{2-9}$$

Here $\{\alpha_k\}$ is a sequence of positive numbers. In applications, most often α_k is chosen identically equal to 1. Through the minimization of equation (2-8), the well-known batch (non-recursive) least squares (LS) coefficient estimation method is obtained [9].

$$\underset{(n+m)\times 1}{\hat{\underline{\theta}}} = \underbrace{\left[\sum_{t=1}^{N}\alpha_t\psi(t)\psi^T(t)\right]^{-1}}_{(n+m)\times(n+m)}\underbrace{\sum_{t=1}^{N}\alpha_t\psi(t)y(t)}_{(n+m)\times 1} \tag{2-10}$$

For on-line parameter estimation purposes, the batch LS method can be rewritten in a recursive fashion, i.e., the recursive LS method [9].

$$\hat{\boldsymbol{\theta}}(t) = \hat{\boldsymbol{\theta}}(t-1) + \boldsymbol{L}(t)[y(t) - \hat{\boldsymbol{\theta}}^T(t-1)\boldsymbol{\psi}(t)] \tag{2-11}$$

$$\boldsymbol{L}(t) = \frac{\boldsymbol{P}(t-1)\boldsymbol{\psi}(t)}{1/\alpha_t + \boldsymbol{\psi}^T(t)\boldsymbol{P}(t-1)\boldsymbol{\psi}(t)} \tag{2-12}$$

$$\boldsymbol{P}(t) = \boldsymbol{P}(t-1) - \frac{\boldsymbol{P}(t-1)\boldsymbol{\psi}(t)\boldsymbol{\psi}^T(t)\boldsymbol{P}(t-1)}{1/\alpha_t + \boldsymbol{\psi}^T(t)\boldsymbol{P}(t-1)\boldsymbol{\psi}(t)} \tag{2-13}$$

To start this recursive algorithm, the initial conditions $\boldsymbol{P}(t_0)$ and $\hat{\boldsymbol{\theta}}(t_0)$ are needed. In [9], it is shown that the proper initial values for the recursive LS method should be given by equations (2-14) and (2-15).

$$\boldsymbol{P}(t_0) = [\sum_{t=1}^{t_0}\alpha_t\boldsymbol{\psi}(k)\boldsymbol{\psi}^T(k)]^{-1} \tag{2-14}$$

$$\hat{\boldsymbol{\theta}}(t_0) = \boldsymbol{P}(t_0)\sum_{t=1}^{t_0}\alpha_t\boldsymbol{\psi}(k)y(k) \tag{2-15}$$

In [9], it is also shown that the relative importance of the initial values decays with time. Therefore, a suggested and common choice of initial values is to take $\boldsymbol{P}(0) = C\cdot\boldsymbol{I}$ and $\hat{\boldsymbol{\theta}}(0) = \boldsymbol{0}$, where C is some large constant.

After obtaining the estimation of model parameters, $\hat{\theta}$, a mapping function f is used to find the physical parameters, $\hat{p}$, of the system.

$$\hat{p} = f^{-1}(\hat{\theta}) \tag{2-16}$$

Through on-line monitoring of the physical parameters of the system, faults can be detected and isolated. However, it has already been shown by Isermann [5] that a unique determination of physical parameters, p, is not always possible. For example, in a first order electrical circuit (see Fig. 2.1), the relation between the output voltage, u_o, and the input voltage, u_i, is

$$RC\frac{du_o}{dt} + u_o = u_i \tag{2-17}$$

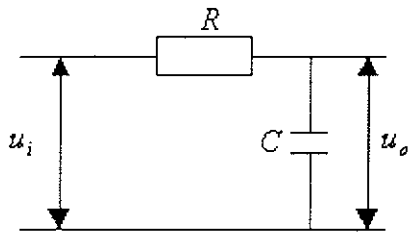

Fig. 2.1 First order electrical circuit.

It is clear that we cannot determine the values of either R or C separately by only measuring the input and output voltage, u_i and u_o. Thus, the faults pertaining either to R or C cannot be isolated.

Another problem with this methodology is that a linear process model that describes the process behavior is sometimes not available and there are no powerful parameter estimation methods for general nonlinear models.

2.2.3 Fault Diagnosis for Systems without Explicit Model

There are many dynamic systems where the physical laws that govern their behavior cannot be easily expressed by mathematical equations. Such systems can only be modeled based on their input and output characteristics through experiments. There exist two distinct relations between the derived model and the physical system. One is the relationship between the system's physical parameters and coefficients of the mathematical model. The other is the relationship between states of the model and the physical state variables of the system. In such cases, the direct implement of either the observer based or the parametric estimation based fault detection and isolation strategy becomes very challenging. In this thesis, a parameter estimation based fault detection and isolation strategy is investigated for hydraulic systems. The general procedure for this methodology is elaborated in the next chapter.

Chapter 3 Fault Detection and Isolation in Feature Space

For systems which can only be modeled based on their input and output characteristics through experiments, the key to model-based fault detection and isolation strategy is to find the relationship between the faults and the changes in the model coefficients. Since the mapping function described by equation (2-16) cannot be easily obtained, the on-line values of system physical parameters cannot be determined. Therefore, the relationship between the faults and the changes in the system physical parameters has to be investigated empirically. The general fault diagnosis procedure based on parameter estimation is illustrated in Fig. 3.1.

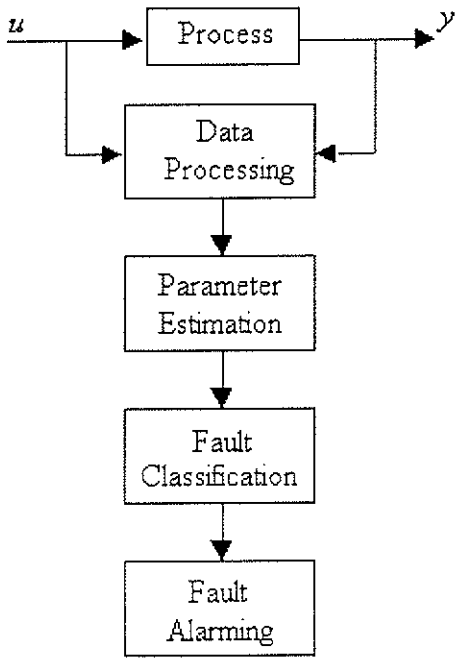

Fig. 3.1 Generalized scheme of fault diagnosis.

3.1 Data Processing

Most monitoring systems are implemented in digital computers. When a monitored process is running, input and output signals are sampled at a time interval, T_s, through a sampling device. Once the measured signals are collected, they may be processed by methods using digital signal processing (DSP) technologies, such as buffering, re-sampling, de-trending or filtering. Therefore, only the most important features of the signals are left for fault detection and isolation.

Buffering collects the consecutive signal samples into a single unit, which is called a batch or frame. By propagating these multi-sample frames instead of the individual signal samples, one can take the speed advantage of execution of DSP algorithm, such as Fast Fourier Transform (FFT). Re-sampling changes the sampling frequency in software. If it turns out that the data has been sampled too fast (which may be required for control purposes) for the monitoring system, they can be decimated. For example, if every k^{th} sample is picked up, the sampling frequency will change to $\frac{f_s}{k}$ from the original sampling frequency, f_s. De-trending the data involves removing the mean values or linear trends from the signal. For a signal such as

$$s(t) = s_0 + A\sin(\omega t + \psi) \tag{3-1}$$

The dc component s_0 may not be of interest. Thus, it is de-trended to

$$s'(t) = A\sin(\omega t + \psi) \tag{3-2}$$

Filtering extracts the most interested frequency components from the sampled signals. It is a good way of removing high frequency noise in the data. It is also a good alternative to de-trending by cutting out low frequencies from the pass band.

3.2 Model Selection and Parameter Estimation

Modeling can provide a direct way to present the characteristics of the monitored system. There are two kinds of system modeling strategies: one is the derivation of the mathematical model from the physical law that governs the behavior of the system, while the other tries to model the system through experiment. Since the only information available to the monitoring system is the input-output set of the monitored process, a mathematical model should be found based on the on-line information of this process. Then parameter estimations can be applied to the selected model structure to get the model coefficients.

3.2.1 Model Selection

The structure of the model determines how the input and output information is formed. For linear structures, autoregressive with exogenous input (ARX), autoregressive moving average with exogenous input (ARMAX), output-error (OE), box-jenkins (BJ) and state-space models [9] are all good candidates. For nonlinear systems, use of an artificial neural network (ANN) is an option.

3.2.1.1 ARX Model

For single-input and single-output systems, the ARX model is the most commonly used model structure. It relates the current output $y(t)$ to a finite number of past outputs $y(t-k)$, inputs $u(t-k)$ and current noise $e(t)$.

$$\begin{aligned} & y(t)+a_1y(t-1)+a_2y(t-2)+\cdots+a_ny(t-n) \\ & =b_1u(t-k)+b_2u(t-k-1)+b_3u(t-k-2)+\cdots+b_mu(t-k-m+1)+e(t) \end{aligned} \tag{3-3}$$

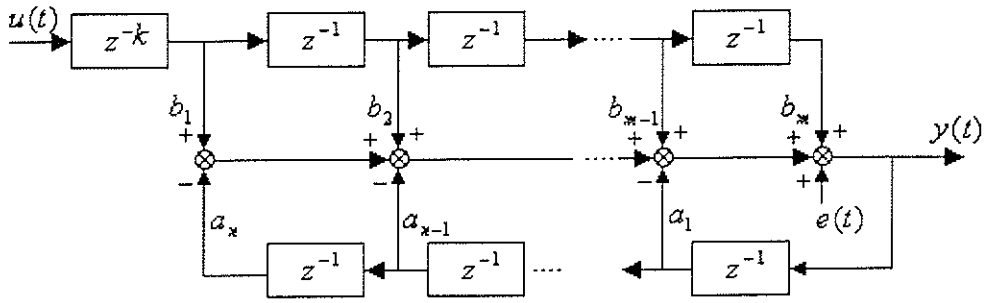

Fig. 3.2 Diagram of ARX model.

In Fig. 3.2, z^{-1} denotes unit time delay. After selecting the values of n, m and k, the structure of the ARX model is determined: n is equal to the number of poles, $m-1$ is the number of zeros and k is the pure time-delay (also called dead-time) in the system. k is equal to 1 if there is no dead-time.

3.2.1.2 ARMAX Model

The difference between the ARMAX model and the ARX model is that in the ARMAX model, the noise, $e(t)$, is also moving-averaged.

$$\begin{aligned} & y(t)+a_1y(t-1)+a_2y(t-2)+\cdots+a_ny(t-n) \\ & =b_1u(t-k)+b_2u(t-k-1)+b_3u(t-k-2)+\cdots+b_mu(t-k-m+1) \\ & +e(t)+c_1e(t-1)+c_2e(t-2)+\cdots+c_le(t-l) \end{aligned} \tag{3-4}$$

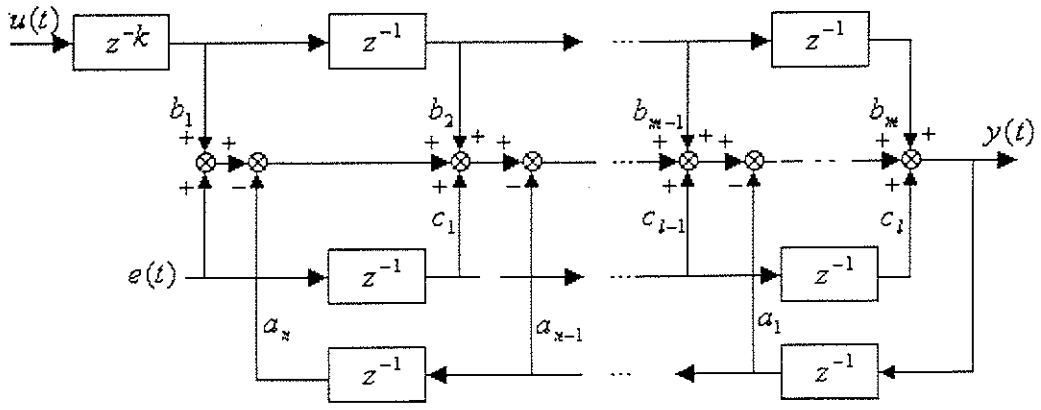

Fig. 3.3 Diagram of ARMAX model.

In this model, n, m, and k have the same meaning as in the ARX model and l is the number of zeros from $e(t)$ to $y(t)$. The structure is determined by the values of n, m, k, and l.

3.2.1.3 Output-Error Model

Instead of treating noise, $e(t)$, as another source of input, the OE model assumes that the noise, $e(t)$, is near the measurement of output, $y(t)$ (see Fig. 3.4).

$$\begin{aligned}&[y(t)-e(t)]+a_1[y(t-1)-e(t-1)]+\cdots+a_n[y(t-n)-e(t-n)]\\&=b_1u(t-k)+b_2u(t-k-1)+b_3u(t-k-2)+\cdots+b_mu(t-k-m+1)\end{aligned} \tag{3-5}$$

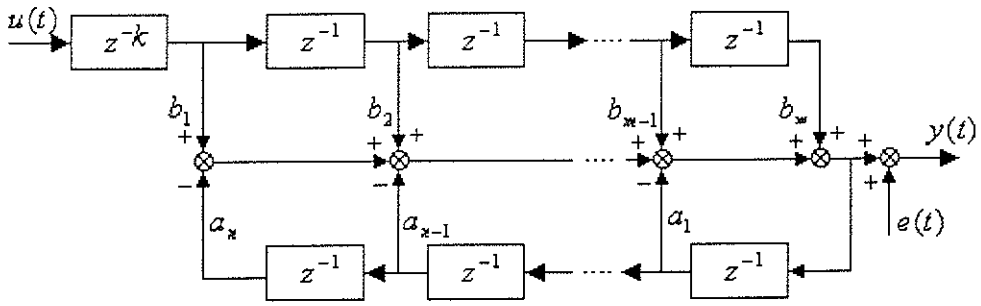

Fig. 3.4 Diagram of Output-Error model.

Similarly to the ARX model, the structure is determined by values of n, m and k.

3.2.1.4 Box-Jenkins Model

The BJ model assumes that input signal, $u(t)$, and noise signal, $e(t)$, affect the output, $y(t)$, through separate channels. Each channel will be output auto-regressive and input moving average. With reference to Fig. 3.5, output $y(t)$ consists of two separate components, $y_1(t)$ and $y_2(t)$.

$$\begin{aligned}&y_1(t)+a_1y_1(t-1)+a_2y_1(t-2)+\cdots+a_{n_1}y_1(t-n_1)\\&=b_1u(t-k_1)+b_2u(t-k_1-1)+b_3u(t-k_1-2)+\cdots+b_{m_1}u(t-k_1-m_1+1)\end{aligned} \tag{3-6}$$

$$y_2(t) + c_1 y_2(t-1) + c_2 y_2(t-2) + \cdots + c_{n_2} y_1(t-n_2)$$
$$= d_1 e(t-k_2) + d_2 e(t-k_2-1) + d_3 e(t-k_2-2) + \cdots + d_{m_2} u(t-k_2-m_2+1) \quad (3\text{-}7)$$

$$y(t) = y_1(t) + y_2(t) \quad (3\text{-}8)$$

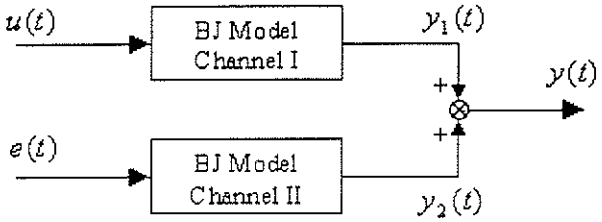

Fig. 3.5 Diagram of Box Jenkins model.

The structure of the BJ model is determined by the values of n_1, m_1, k_1, n_2, m_2 and k_2.

3.2.1.5 State Space Model

For multiple-input-multiple-output (MIMO) systems, the state space model is a good choice. The basic state-space model (see Fig. 3.6) is written as

$$\boldsymbol{x}(t+1) = \boldsymbol{A}\boldsymbol{x}(t) + \boldsymbol{B}\boldsymbol{u}(t) + \boldsymbol{K}e(t)$$
$$\boldsymbol{y}(t) = \boldsymbol{C}\boldsymbol{x}(t) + \boldsymbol{D}\boldsymbol{u}(t) + e(t) \quad (3\text{-}9)$$

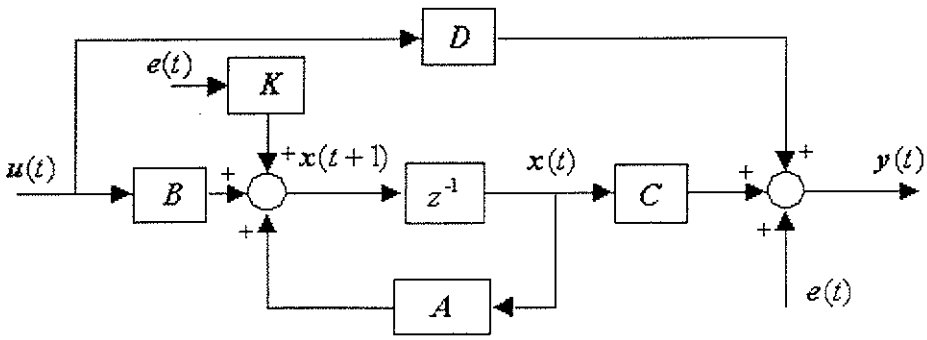

Fig. 3.6 Diagram of state space model.

The most important value to determine in the state space model is the dimension of the state vector, $\boldsymbol{x}(t)$. The state space model has several derivatives. If $\boldsymbol{K} = \boldsymbol{0}$, an

Output-Error model is defined. If $D = 0$, there exists at least a delay of one sample from the input to the output.

3.2.1.6 Artificial Neural Network Model

A neural network is a collection of interconnected neurons. Each neuron's operation is quite simple, as illustrated in Fig. 3.7.

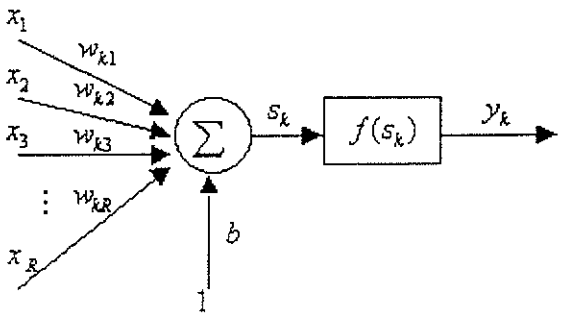

Fig. 3.7 Schematic of single neuron.

Vector $x^T = [x_1, x_2, x_3, \cdots, x_R]$ is the input vector. $w_k = [w_{k1}, w_{k2}, w_{k3}, \cdots, w_{kR}]$ is the weight vector and b is the bias, which acts as a weight except that it has a constant input of 1.

$$s_k = \sum_{i=1}^{R} w_{ki} x_i + b = \boldsymbol{w}_k \boldsymbol{x} + b \tag{3-10}$$

f is the activation function. The output of the neuron is a function of s_k.

$$y_k = f(s_k) = f(\boldsymbol{w}_k \boldsymbol{x}_k + b) \tag{3-11}$$

Two or more neurons may be combined in one layer and a neural network might contain one or more such layers. The layer where neurons receive inputs directly from outside of the network is called the input layer. A layer that produces the network's output is called an output layer. All other layers are called hidden layers.

Depending on the input data structure, neural network can be divided into two types. If the input vectors are given without considering a particular time sequence, the network is called a static network. If the input vectors occur sequentially with time, the network is called a dynamic network, which is a better choice than a static network for representing the dynamic behavior of the system. According to the direction of the signal flow, neural networks can also be classified as feed-forward or feedback networks. To represent temporal behavior, internal feedback paths may be required.

The structure of an artificial neural network is very flexible, which is determined by the number of network layers, the number of neurons in each layer, the type of activation function in each layer and how the layers are connected with each other. The best architecture to use depends on the type of problem to be represented by the network.

3.2.1.7 Model Selection Criteria

Several model structures have been introduced above. For the purposes of fault detection and isolation, there are several important criteria to be observed in model selection:

1. Given a model structure, powerful on-line model coefficient estimation methods should be available. From this point of view, artificial neural networks are not a good choice since they need time to converge.
2. The estimated model can approximate the behavior of the monitored system as closely as possible.
3. The variances of the estimated coefficients affect the resolution of the fault detection. For any specific parameter value, they should be as small as possible.

All these criteria are essential to the fault detection and isolation strategy discussed in this work.

3.2.2 Parameter Estimation for Fault Diagnosis

After selecting a proper model, the input and output relationship can be expressed as

$$y(t) = f(\psi(t), \theta) \tag{3-12}$$

where $\psi(t)$ is a matrix; its elements are composed of

$$u(t-k), u(t-k-1), \cdots, u(t-k-m+1), y(t-1), y(t-2), \cdots, y(t-n)$$

θ is the parameter vector; its elements are the coefficients to be estimated. For example, an ARX model as described in (3-3) can be expressed as follows:

$$\psi^T(t) = \left[-y(t-1), -y(t-2), \cdots, -y(t-n), u(t-k), \cdots, u(t-k-m+1)\right] \tag{3-13}$$

$$\theta^T = [a_1, a_2, \cdots, a_n, b_1, b_2, \cdots, b_m] \tag{3-14}$$

$$y(t) = \theta^T \psi(t) + e(t) \tag{3-15}$$

With the help of parameter estimation algorithms, the model coefficients, θ, can be estimated. From the viewpoint of fault detection and isolation, two definitions are presented here:

1. If a change in system physical parameter does not alter the value of θ, this change cannot be detected for the selected model structure.
2. If changes in more than one parameter affect the value of θ in the same manner, these two faults cannot be isolated.

To solve the problem of either case 1 or case 2, one way is to change the order of the model. Alternatively, one may use a different model structure.

3.3 Fault Classification

As far as fault detection and isolation are concerned, the value of θ can be divided into normal and faulty ranges. Depending upon the type of fault, the faulty ranges can be further classified as fault I, fault II and so on. The task of the monitoring system is to reach the decision surface among these ranges and make a classification when an unknown sample is presented.

If the new sample is classified to the fault I group, the monitoring system assumes that fault I has occurred. It can express this information in various forms, such as ringing an alarm bell. The procedure of how to correct the fault condition is specific to different kinds of application and will not be addressed here.

3.5 Summary

In this chapter, the procedure for fault detection and isolation, based on parameter estimation, has been outlined. The implementation of this strategy involves model selection, parameter estimation and fault classification and training. Other model-based fault detection and isolation methods, such as unknown input observer and physical parameter estimation, require explicit mathematical model from physical laws. This strategy mainly relies on on-line information of input and output signals from the monitored process. In the subsequent chapters, this strategy will be tested on a double-rod hydraulic actuator in both simulations and experiments.

Chapter 4 Model of Electrohydraulic Actuators

Hydraulic actuators may be linear or rotary and are usually referred to as pistons or motors, respectively. A pump or a valve can be used to control these actuators. The pump-controlled system consists of a variable delivery pump supplying fluid to the actuating device. The fluid flow is controlled by the stroke of the pump to vary output speed and the generated pressure matches the load. The valve-controlled system consists of a servovalve controlling the flow from a hydraulic power supply to the actuating device. As compared with pump-controlled hydraulic actuators, valve-controlled actuators have faster response capability; this makes them the preferred choice in the majority of applications [8].

A diagram of a double-rod valve-controlled electrohydraulic actuator is shown in Fig. 4.1. It consists of a hydraulic power supply, an electrohydraulic valve, a rod and a cylinder. The function and dynamic characteristics of each part will be explained in the following sections.

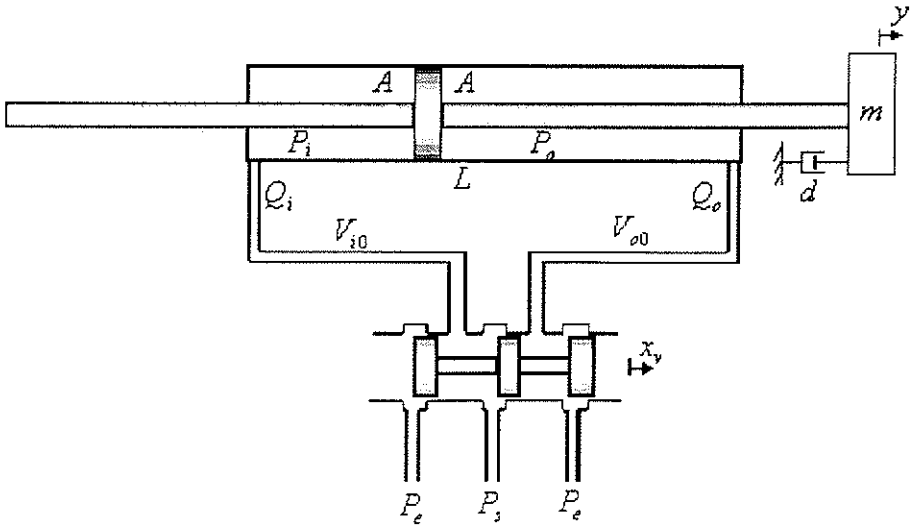

Fig. 4.1 Schematic of a valve-controlled hydraulic actuator.

4.1 Power Supply

The hydraulic power supply is usually a constant pressure type. There are two kinds of configuration: one consists of a constant delivery pump with a relief valve to regulate pressure; the other uses a variable pump with a stroke control to regulate pressure. The function of this pump unit is to provide hydraulic supply fluid with a constant pressure, as shown by P_s in Fig.4.1.

4.2 Servovalve

Hydraulic control valves are devices that use mechanical motion to control fluid power. The most widely used valve is the sliding valve employing a spool type construction. Spool valves are classified by:

1. The number of "ways" flow can enter and leave the valve.
2. The number of "lands".
3. The type of center when the valve spool is in the neutral position. If the width of the land is smaller than the port in the valve sleeve, the valve is said to be under-lapped. A critical center or zero-lapped valve has a land width identical to the port width. Overlapped valves have a land width greater than the port width when the spool is at neutral.

In Fig. 4.1, a three-land-four-way spool valve with a critical center is shown. Since the versatility of electrical devices makes them ideal for feedback measurement and signal amplification and manipulation, the mechanical motion of the valve is controlled by an electrical signal; such a valve is called an electrohydraulic servovalve. It converts low power electrical signals into valve motion, which in turn controls the flow to a

hydraulic actuator. Electrohydraulic servovalves can be broadly classified as either single-stage or two-stage. A single-stage servovalve consists of a torque motor that is directly attached to and positions a spool valve. Because torque motors have limited power capability, this in turn limits the flow capacity of the single-stage servovalve and may also lead to stability problems in some applications. A two-stage servovalve has a hydraulic preamplifier (called first stage) that substantially multiplies the force output of the torque motor to a level sufficient to overcome the considerable flow forces, sticking forces, and forces resulting from acceleration or vibration. The two-stage servovalve overcomes both of the disadvantages of single-stage servovalve and this is the main reason for their existence.

Many design factors and operational and environmental variables make it very difficult to assume an explicit linear transfer function for an electrohydraulic servovalve. However, the usefulness of linear transfer functions in approximating servovalve responses in analytical studies is well established. The relationship between the valve spool displacement, x_v, and the input voltage, u, to the valve can be expressed by the following differential equation [11]:

$$\frac{d^2 x_v}{dt^2} + 2\xi\omega_n \frac{dx_v}{dt} + \omega_n^2 x_v = K_v \omega_n^2 u \tag{4-1}$$

where ω_n is the natural frequency, ξ is the damping ratio and K_v is the servovalve loop gain.

4.3 Fluid Flow Dynamic

The valve spool displacement, x_v, controls the orifices through which fluid power enters and leaves the hydraulic cylinder. Assuming that the valve orifices are matched,

symmetrical and rectangular ports with an area gradient of w for each port are used, the fluid flow dynamic in Fig. 4.1 is expressed as

$$x_v \geq 0 \begin{cases} Q_i = C_d w x_v \sqrt{\frac{2}{\rho}(P_s - P_i)} \\ Q_o = C_d w x_v \sqrt{\frac{2}{\rho}(P_o - P_e)} \end{cases} \tag{4-2}$$

$$x_v < 0 \begin{cases} Q_i = C_d w x_v \sqrt{\frac{2}{\rho}(P_i - P_e)} \\ Q_o = C_d w x_v \sqrt{\frac{2}{\rho}(P_s - P_o)} \end{cases} \tag{4-3}$$

where C_d is the discharge coefficient and ρ is the mass density of fluid.

For the control volume shown in Fig. 4.2, there are weight flow rates W_{in} into and W_{out} out of it. The accumulated fluid has volume V, mass m and mass density ρ. From the law of conservation of mass, the rate at which mass is stored must be equal to the incoming mass flow rates minus the outgoing mass flow rates, i.e.:

$$g\frac{dm}{dt} = g\frac{d\rho V}{dt} = W_{in} - W_{out} \tag{4-4}$$

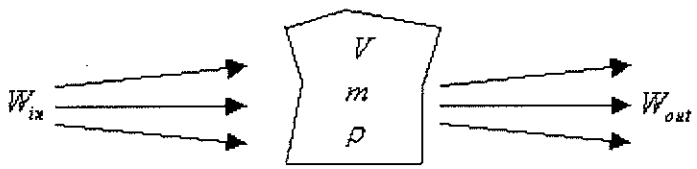

Fig. 4.2 Flows entering and leaving a control volume.

Isothermal conditions are generally assumed in the liquid flow. Thus, the fluid mass density ρ can be expressed as

$$\rho = \rho_0 + \frac{\rho_0}{\beta} P \tag{4-5}$$

where ρ_0 and β are the fluid mass density and bulk modulus at zero pressure, and P is the current flow pressure. Noting that the weight flow rate can be written as

$$W_{in} = g\rho Q_{in} \tag{4-6}$$

$$W_{out} = g\rho Q_{out} \tag{4-7}$$

Equation (4-4) can be rewritten as:

$$g\rho Q_{in} - g\rho Q_{out} = g\rho \frac{dV}{dt} + \frac{gV\rho_0}{\beta} \frac{dP}{dt} \tag{4-8}$$

Taking $\rho \approx \rho_0$, equation (4-8) can be expressed as

$$Q_{in} - Q_{out} = \frac{dV}{dt} + \frac{V}{\beta} \frac{dP}{dt} \tag{4-9}$$

Referring to Fig. 4.1, for fluid trapped in the left side of the cylinder,

$$V_i = V_{i0} + Ay \tag{4-10}$$

For fluid trapped in the right side of the cylinder,

$$V_o = V_{o0} + A(L - y) \tag{4-11}$$

where V_{i0} and V_{o0} are the initial volumes trapped on the left and right sides of the cylinder, respectively, and L is the length of the full stroke. The pressure dynamic equations can be expressed as:

$$\frac{dP_i}{dt} = \frac{\beta}{V_{i0} + Ay} (Q_i - A\frac{dy}{dt}) \tag{4-12}$$

$$\frac{dP_o}{dt} = \frac{\beta}{V_{o0} + A(L - y)} (-Q_o + A\frac{dy}{dt}) \tag{4-13}$$

4.4 Piston Dynamic

By applying Newton's Second Law to the forces on the piston, the piston dynamic can be expressed as

$$v = \dot{y} \tag{4-14}$$

$$m\dot{v} = P_i A - P_o A - dv \tag{4-15}$$

where m is the mass of the load, d is the equivalent viscous damping coefficient, y is the displacement of the rod, v is the speed of the rod, and A is the piston area at both sides of the cylinder.

4.5 Summary

In this chapter, different parts of the electrohydraulic actuator shown in Fig. 4.1 were explained. By using the state vector $x^T = [x_1, x_2, \cdots, x_6] = [y, v, P_i, P_o, x_v, \dot{x}_v]$ to represent the physical states of the hydraulic actuator, the dynamic equations used to describe the actuator can be summarized as

$$\begin{cases} \dot{x}_1 = x_2 \\ \dot{x}_2 = \dfrac{1}{m}(-dx_2 + Ax_3 - Ax_4) \\ \dot{x}_3 = \dfrac{\beta}{V_{i0} + Ax_1}(-Ax_2 + Q_i) \\ \dot{x}_4 = \dfrac{\beta}{V_{o0} + A(L - x_1)}(Ax_2 - Q_o) \\ \dot{x}_5 = x_6 \\ \dot{x}_6 = -2\xi\omega_n x_6 + \omega_n^2 x_5 + K_v \omega_n^2 u \end{cases} \tag{4-16}$$

$$x_5 \geq 0 \begin{cases} Q_i = C_d w x_5 \sqrt{\frac{2}{\rho}(P_s - x_3)} \\ Q_o = C_d w x_5 \sqrt{\frac{2}{\rho}(x_4 - P_e)} \end{cases} \tag{4-17}$$

$$x_5 < 0 \begin{cases} Q_i = C_d w x_5 \sqrt{\frac{2}{\rho}(x_3 - P_e)} \\ Q_o = C_d w x_5 \sqrt{\frac{2}{\rho}(P_s - x_4)} \end{cases} \tag{4-18}$$

Chapter 5 Simulation Results

In order to illustrate the general fault detection and isolation strategy outlined in Chapter 3, simulations are performed on the double rod electrohydraulic actuator model presented in Chapter 4 for incorrect supply pump pressure and changes in equivalent viscous damping coefficient. The parameter of the hydraulic actuator is listed in Table 5.1.

Table 5.1 Parameters of the electrohydraulic actuator.

C_d	0.60	
ρ	8.47×10^{2}	kg/m^3
w	2.07×10^{-2}	m
ξ	0.70	
ω_n	6.28×10^{2}	rad/s
K_v	2.79×10^{-5}	m/v
L	0.61	m
β	6.89×10^{8}	Pa
P_s	6.89×10^{6}	Pa
P_e	0	Pa
A	6.33×10^{-4}	m^2
d	1000.00	N/(m/s)
m	50.00	Kg

The model selection criteria, feature space formation and fault representation are explained in detail. In the simulation program, the continuous model described by equation (4-16) is solved using a fourth-order Runge-Kutta numerical integration [10]. The integration time interval, h, is set to 1 ms and the initial physical states of the hydraulic system are set as: $y_0 = 0.305$ m, $v_0 = 0$ m/sec, $P_{l0} = P_{s0} = \frac{P_s}{2}$ and $x_{v0} = 0$ m. The configuration of the control system and the monitoring system is demonstrated in Fig. 5.1.

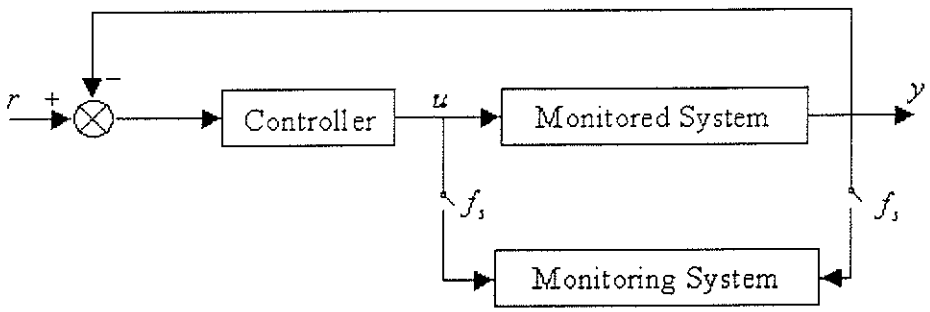

Fig. 5.1 System configuration.

In Fig. 5.1, r is the reference signal. It is set as

$$r(t) = A\sin(2\pi ft) + y_0 \tag{5-1}$$

where A is the amplitude of the reference signal set as 0.0254 m and f is the frequency of the reference signal whose value is set to 0.5 Hz. A proportional controller is applied in the control system. Since most functional fault detection and isolation systems are implemented in digital computers [3], the input signals to the monitoring system have to be sampled. The sampling frequency for both control and monitoring purposes is 200 Hz. The relationship between the continuous reference signal, $r(t)$, and the sampled reference signal, $r(n)$, is expressed in equation (5-2).

$$r(n) = r(nT_s) = A\sin(2\pi\frac{f}{f_s}n) + x_0 \tag{5-2}$$

A typical reference signal, r, control signal, u, and displacement, y, are presented in Figs. 5.2 to 5.4.

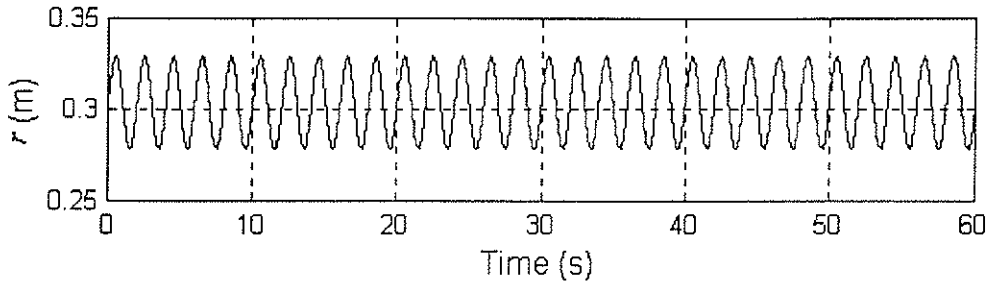

Fig. 5.2 Reference signal.

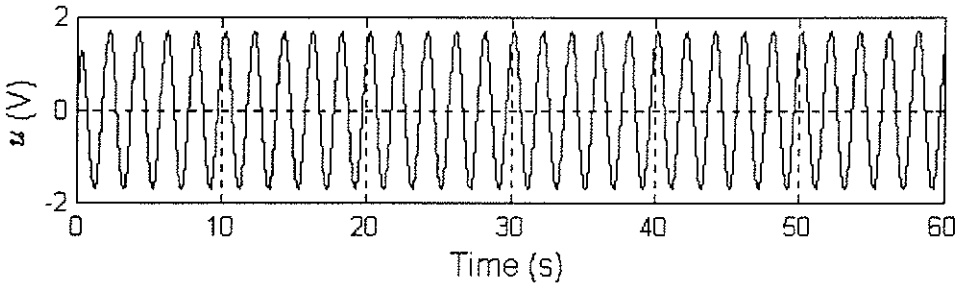

Fig. 5.3 Control signal.

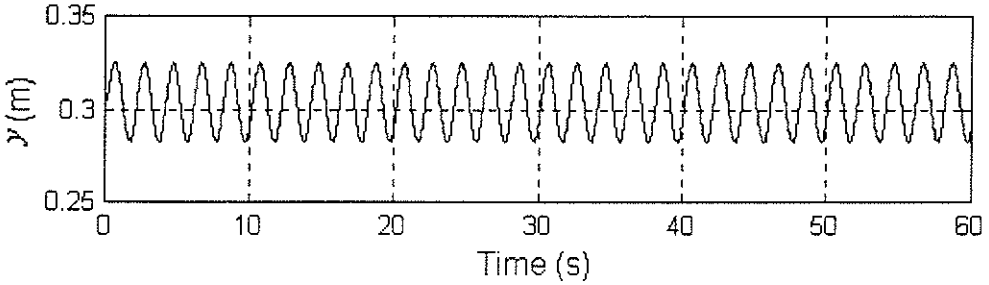

Fig. 5.4 Rod displacement.

The signals used for monitoring purposes are the control signal, u, and the rod displacement signal, y.

5.1 Model Selection

Since the offset component $y = 0.305$ m plays an unimportant role in describing how the changes in the input, u, affects the output, y, it can be de-trended out from the output signal, y. In addition, the three main criteria in selecting the model structure, as stated in Section 3.2.1, are considered. Firstly, there should be powerful model coefficient estimation methods. From this point of view, a linear model is the first choice. Among all linear models described in Section 3.2.1, the ARX model is the most widely used one and is chosen here. It has the following structure:

$$\begin{aligned} &y(t) + a_1 y(t-1) + a_2 y(t-2) + \cdots + a_n y(t-n) \\ &= b_1 u(t-k) + b_2 u(t-k-1) + b_3 u(t-k-2) + \cdots + b_m u(t-k-m+1) + e(t) \end{aligned} \tag{5-3}$$

With different values of m, n and k, different ARX models can be constructed: these are represented by ARXnmk in subsequent sections. In order to select a good model for the system, ARX models with different parameter sets are tried. The data used for model selection purpose is the fifth period of the signals, which is shown in Fig. 5.5. The batch LS algorithm described by equation (2-10) is implemented on this data set to estimate the models' coefficients. In order to investigate the suitability of a specific model, the model is simulated with the same control signal as in Fig. 5.5 and the cost function

$$E = \sum_{n=0}^{N-1} e^2(n) \tag{5-4}$$

is evaluated for this model. With reference to equation (5-4), $e(n)$ is the error signal between the system and model outputs and N is the number of samples evaluated. The model output, y, and error signal, e, for various ARX models are shown in Figs. 5.6 to 5.15.

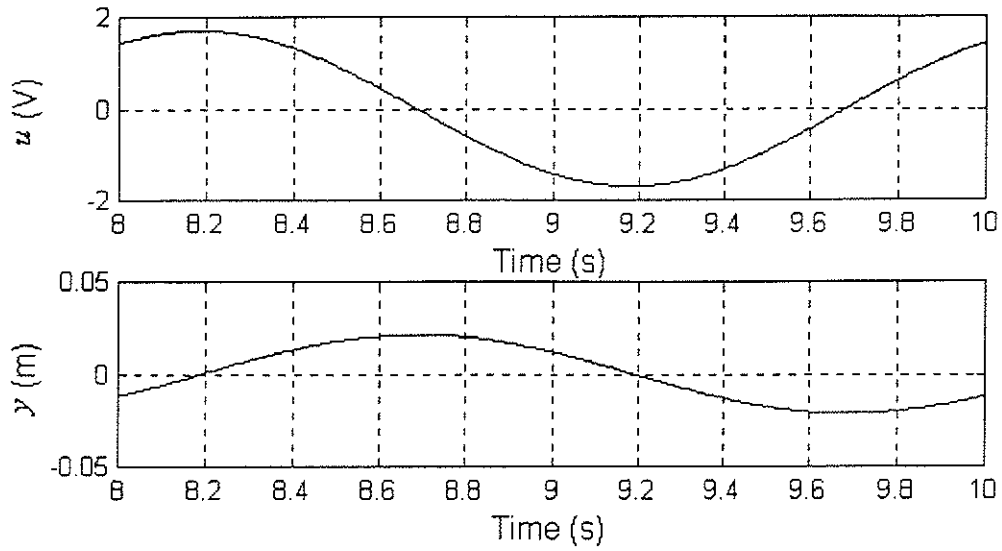

Fig. 5.5 Input and output data pairs for model selection.

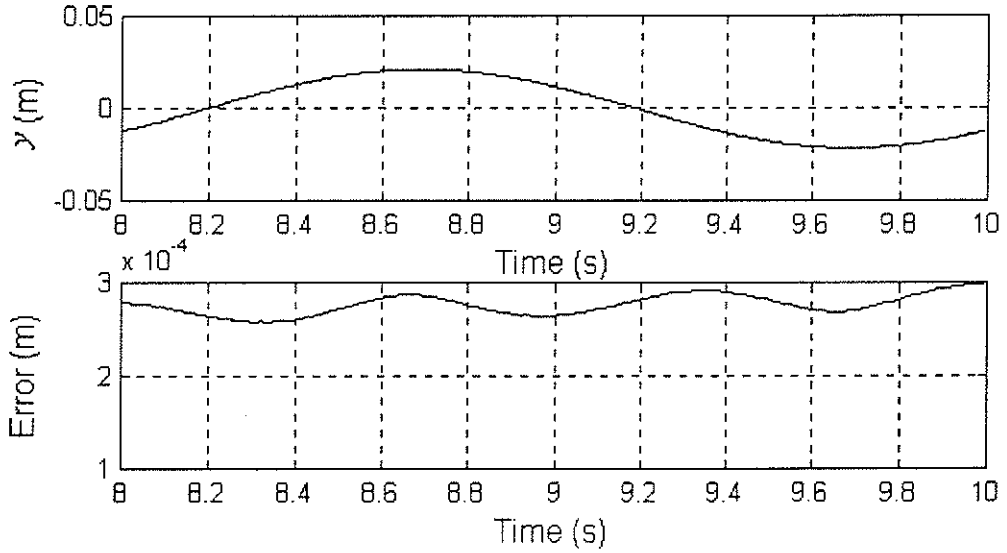

Fig. 5.6 Output and error signals of ARX111 model.

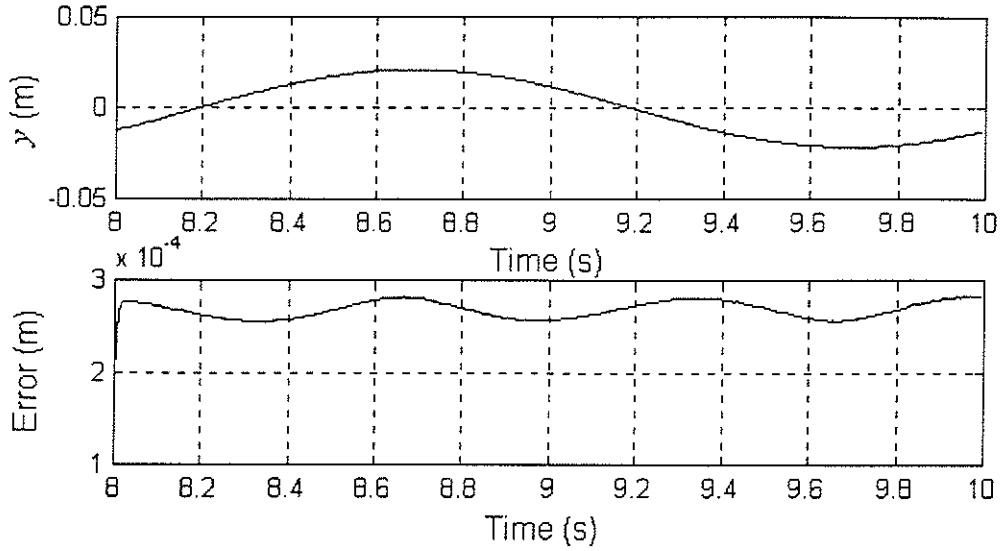

Fig. 5.7 Output and error signals of ARX211 model.

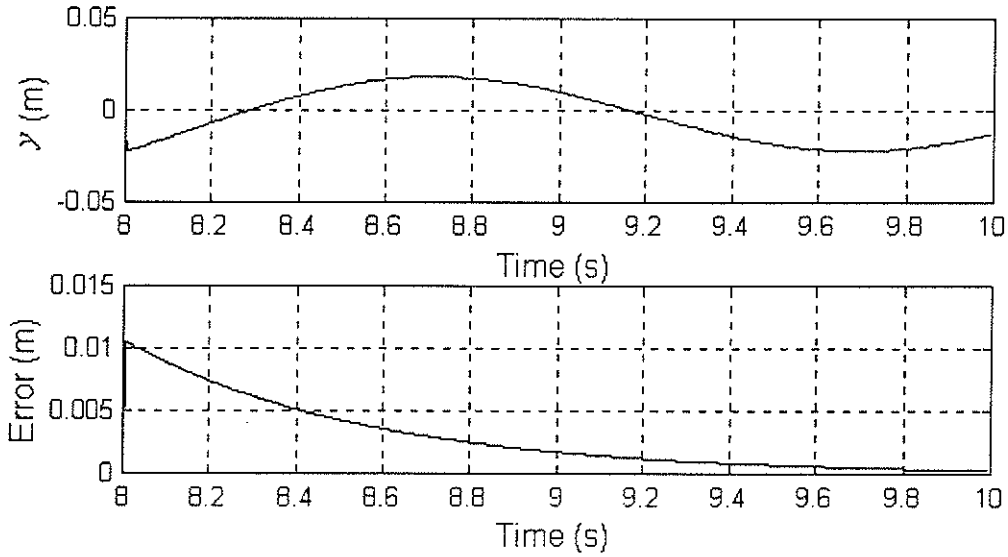

Fig. 5.8 Output and error signals of ARX221 model.

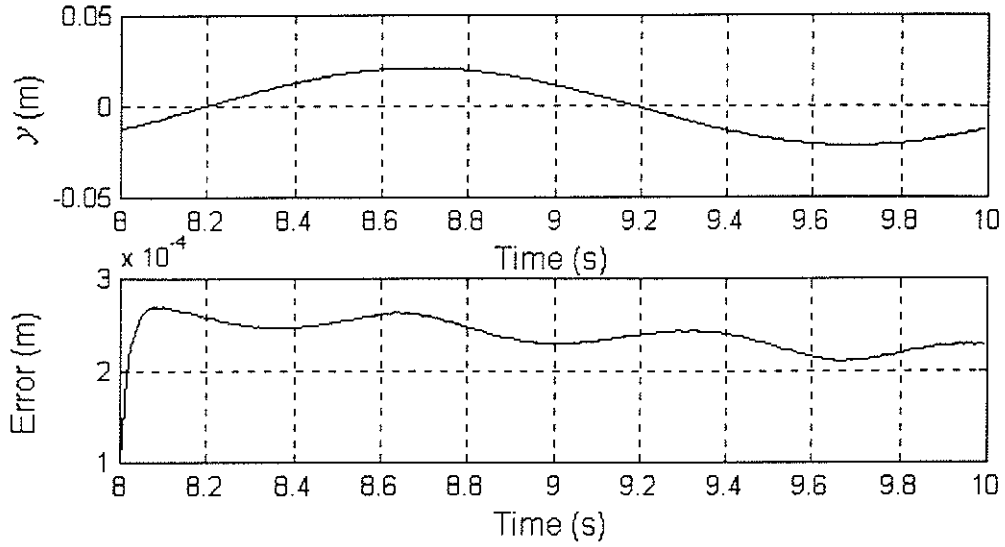

Fig. 5.9 Output and error signals of ARX311 model.

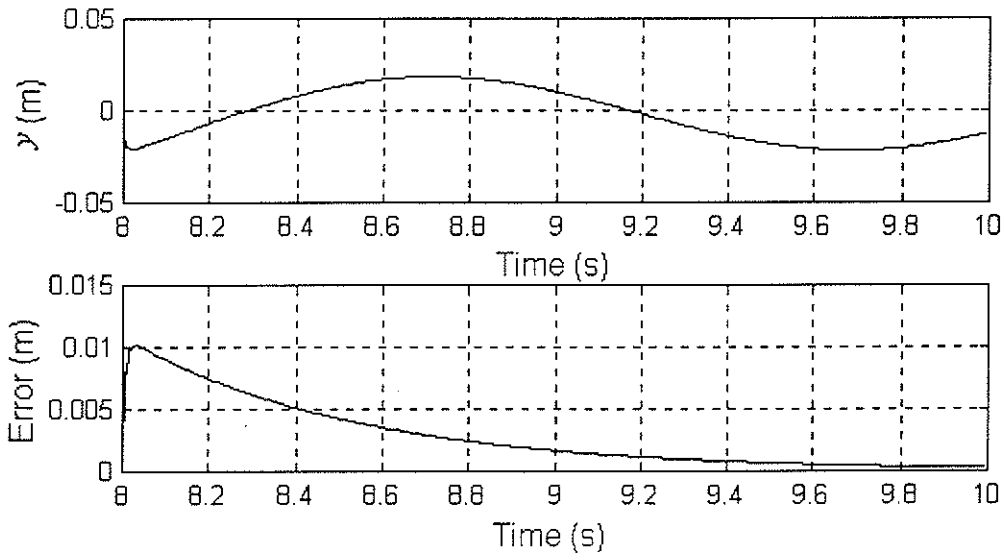

Fig. 5.10 Output and error signals of ARX321 model.

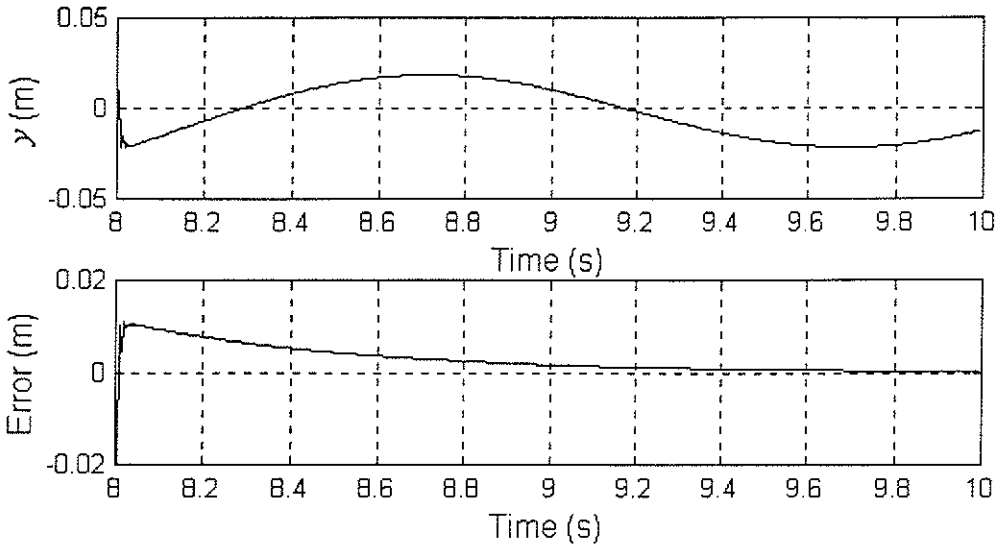

Fig. 5.11 Output and error signals of ARX331 model.

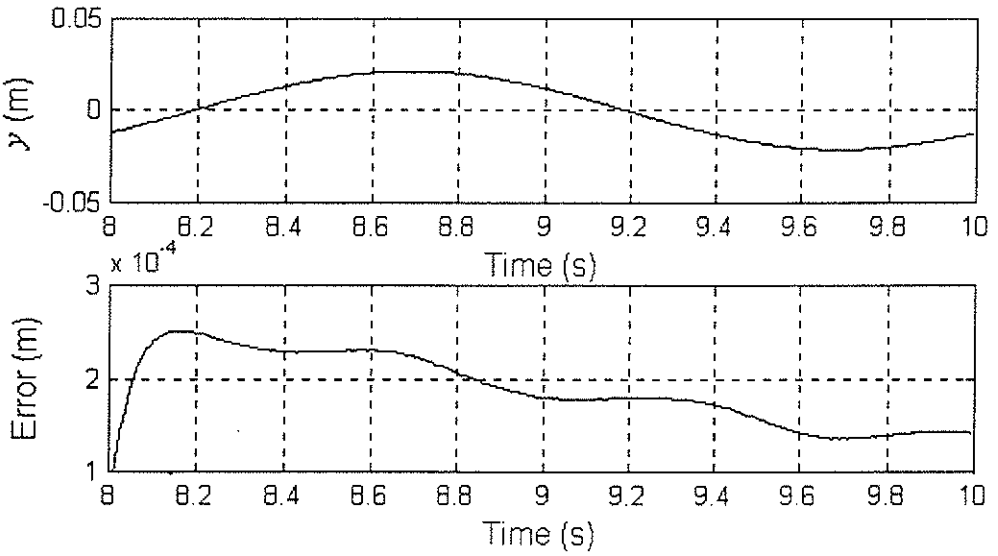

Fig. 5.12 Output and error signals of ARX411 model.

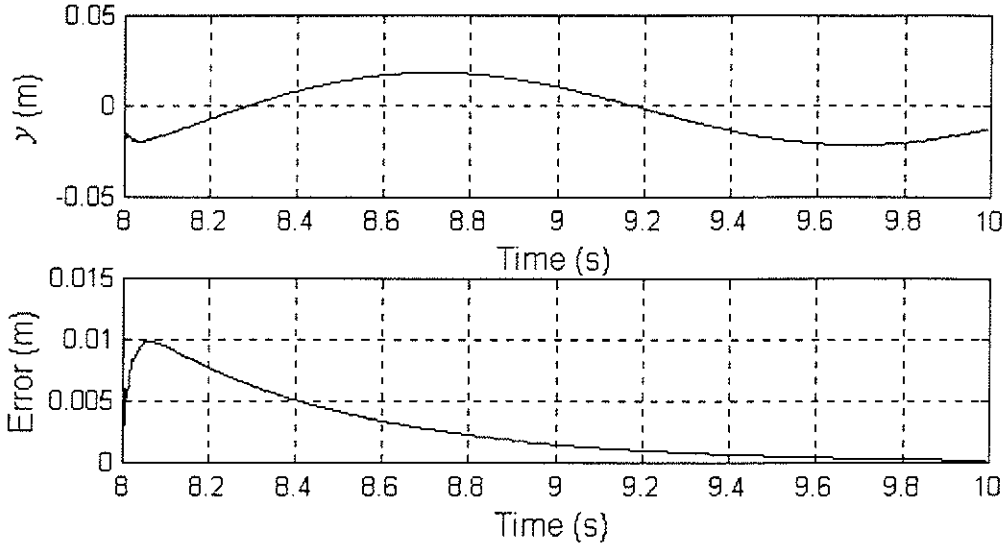

Fig. 5.13 Output and error signals of ARX421 model.

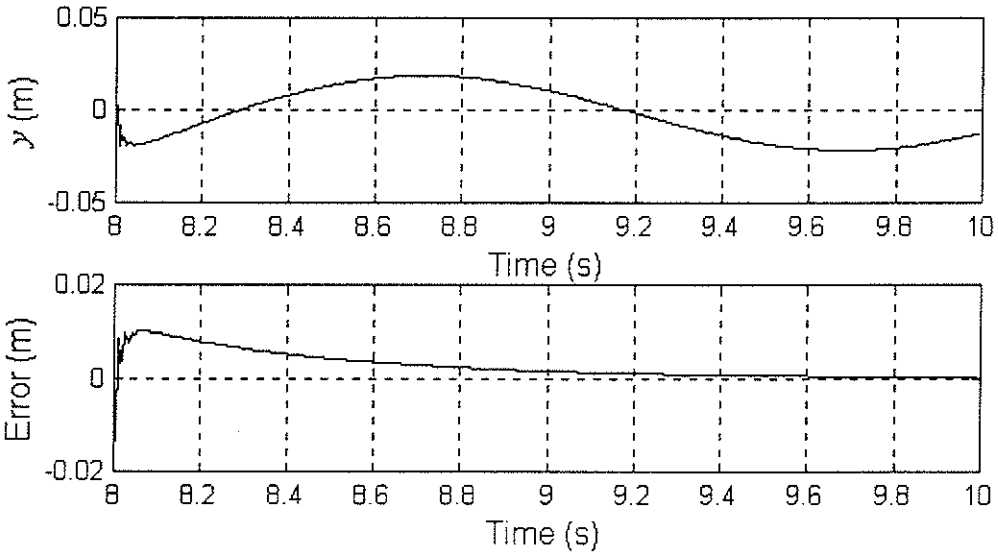

Fig. 5.14 Output and error signals of ARX431 model.

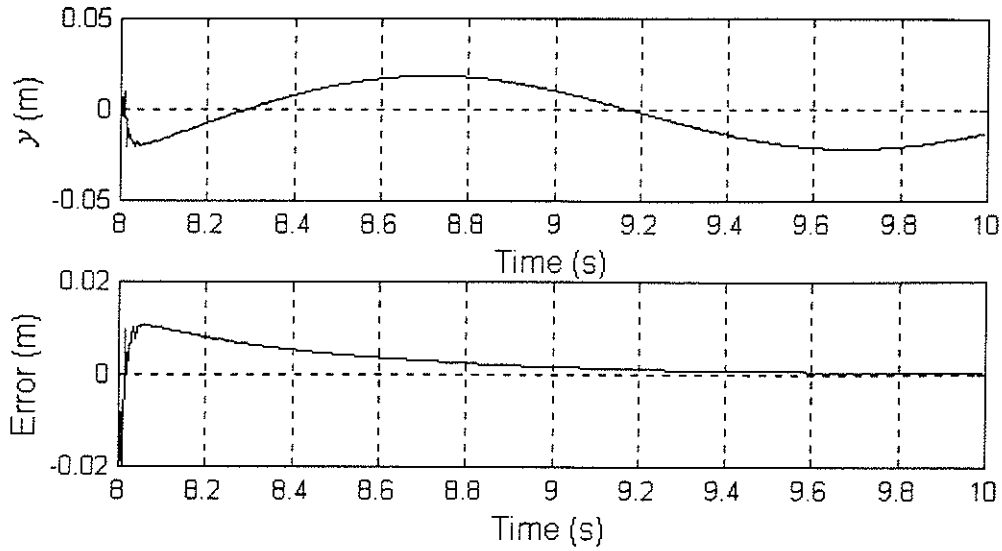

Fig. 5.15 Output and error signals of ARX441 model.

With reference to Figs. 5.6 to 5.15, it is seen that models ARX111, ARX211, ARX311 and ARX411 are all good models to represent the input and output relationship for the system. Table 5.2 shows the cost function values, E, for all the models mentioned above.

Table 5.2 Cost function values for different models.

Model	$E(m^2)$
ARX111	3.04986×10^{-5}
ARX211	2.87777×10^{-5}
ARX221	6.16856×10^{-3}
ARX311	2.29337×10^{-5}
ARX321	6.08998×10^{-3}
ARX331	6.65183×10^{-3}
ARX411	1.48142×10^{-5}
ARX421	5.93432×10^{-3}
ARX431	6.17225×10^{-3}
ARX441	6.89262×10^{-3}

From Table 5.2, it can be seen that, for models ARXn11, the larger the n, the less the E. As stated in Section 3.2.1, in the feature space, the variances of the estimated coefficients reflect the distribution of the points corresponding to system operation conditions. These should be as small as possible. This criterion is now examined by comparing coefficients of the ARX411 model (which has the smallest value of E for the listed ARXn11 models) with those of the ARX111 model (which has the largest value of E for the listed ARXn11 models). The coefficients of these two models are estimated using the batch LS method described in equation (2-10), when the monitoring system collects all the data for each new period. When supply pump pressure is at 900 psi, 1,000 psi and 1,100 psi, the coefficient sets are plotted according to time in Figs. 5.16 and 5.17.

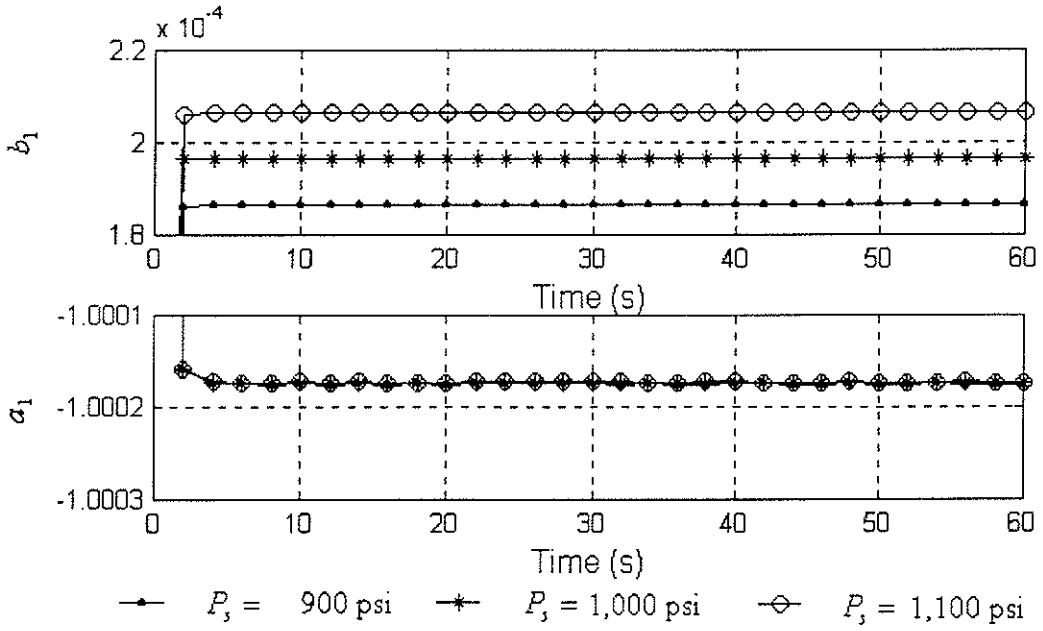

Fig. 5.16 Coefficients of ARX111 model for various supply pump pressures.

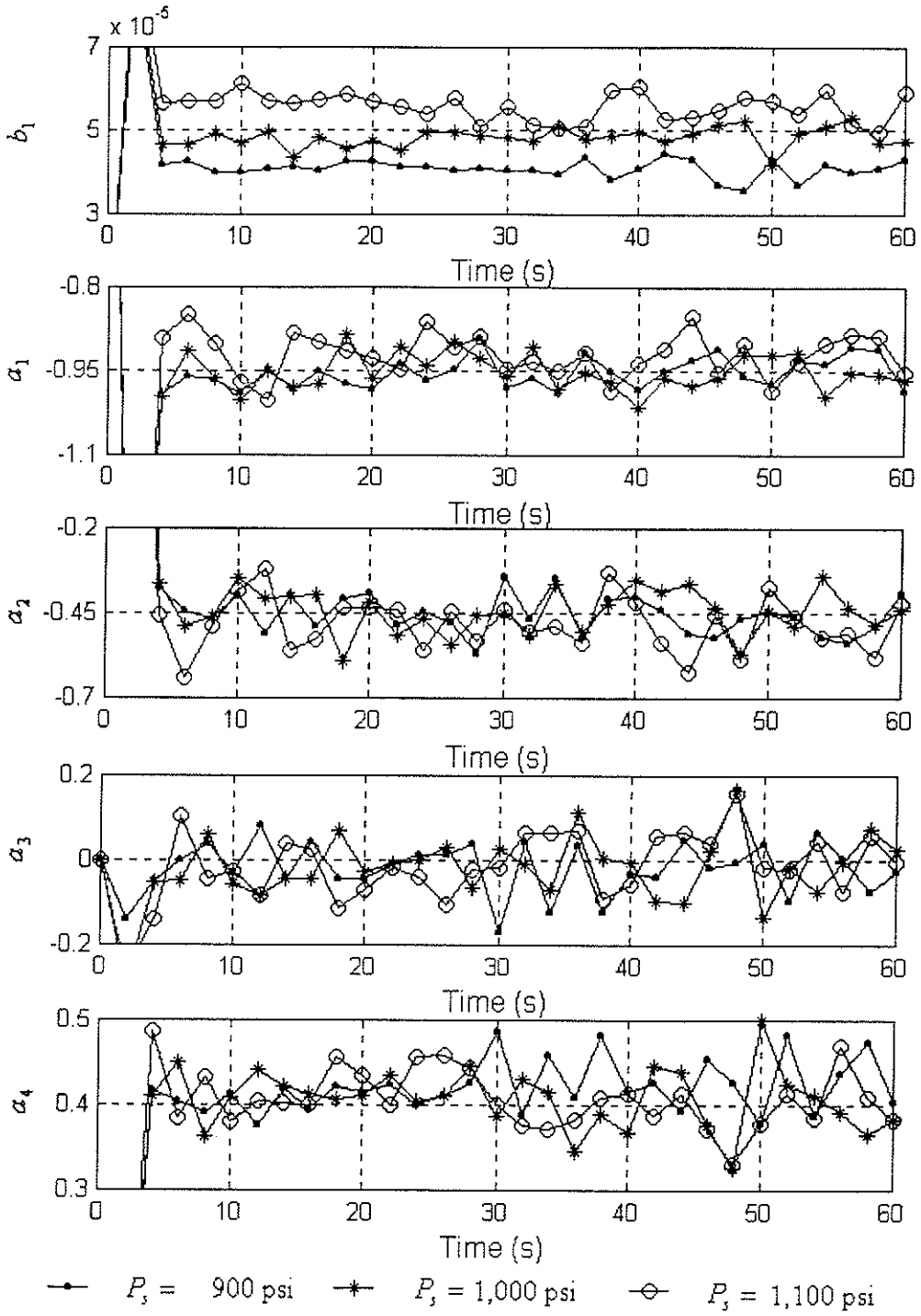

Fig. 5.17 Coefficients of ARX411 model for various supply pump pressures.

For the ARX411 model, shown in Fig. 5.17, it is impossible to distinguish the three operation conditions through threshold checking on a_1, a_2, a_3 or a_4, because they are

interlacing with each other for the conditions under consideration. Although b_1 reflects the change of supply pump pressure more effectively than a_1, a_2, a_3 or a_4, it is still difficult to select a proper threshold value to identify these three conditions without leading to incidental false alarming and/or fault missing. For the ARX111 model, Fig. 5.16 shows that when supply pump pressure changes by $\pm 10\%$, b_1 changes by around $\pm 5\%$. The change of a_1, however, is less than $\pm 0.01\%$. Therefore, threshold checking on b_1 for the ARX111 model can be selected as the fault detection and isolation logic. Fig.5.16 also shows that it is easy to select a proper threshold value on b_1 to clearly distinguish between the considered conditions without false alarming and fault missing. It is seen that, for fault detection and isolation purposes, a compromise has to be made between reducing the value of the cost function, E, and achieving small variances of the estimated model coefficients in model selection. The ARX111 model, therefore, is selected as the best fit model for the hydraulic system under consideration.

5.2 Recursive LS Method versus Batch LS Method

In the batch LS method, the samples are buffered together, after which equation (2-10) is used to estimate coefficients. In the recursive LS method described by equation (2-11), the estimated coefficients are adjusted with each new sample. A detailed description of the batch LS and recursive LS algorithms is provided in [13]. Both methods provide good performance for linear time-invariant (LTI) systems. For nonlinear systems with changing operating point, however, when a linear model to represent the system dynamic characteristics, the recursive LS method may lead to results with larger variance than the batch LS method.

To study the difference between these methods, the ARX111 model output, error signal (between system and model outputs) and estimated coefficients using the batch LS method and the recursive LS method for supply pump pressure at 1,000 psi are shown in Figs. 5.18 to 5.21.

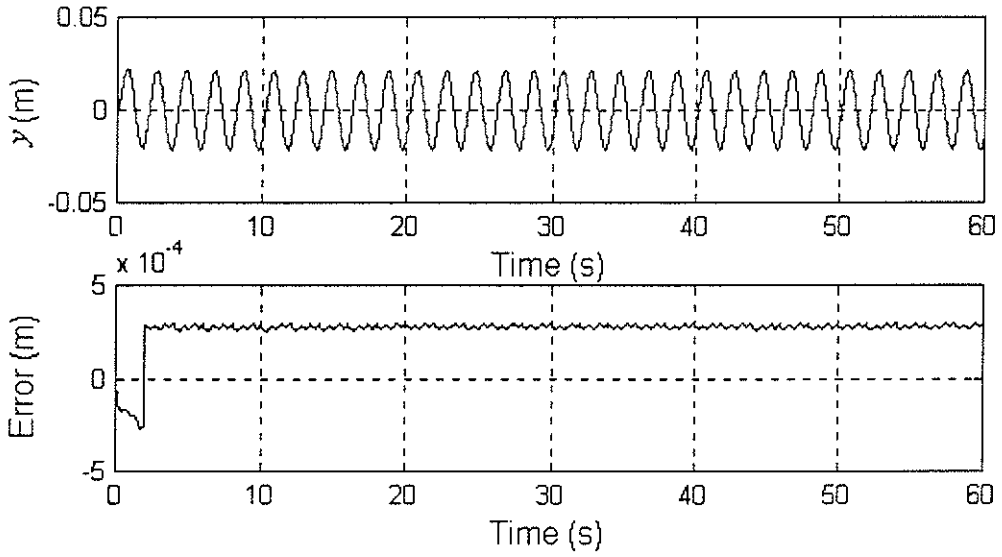

Fig. 5.18 ARX111 model output using the batch LS method.

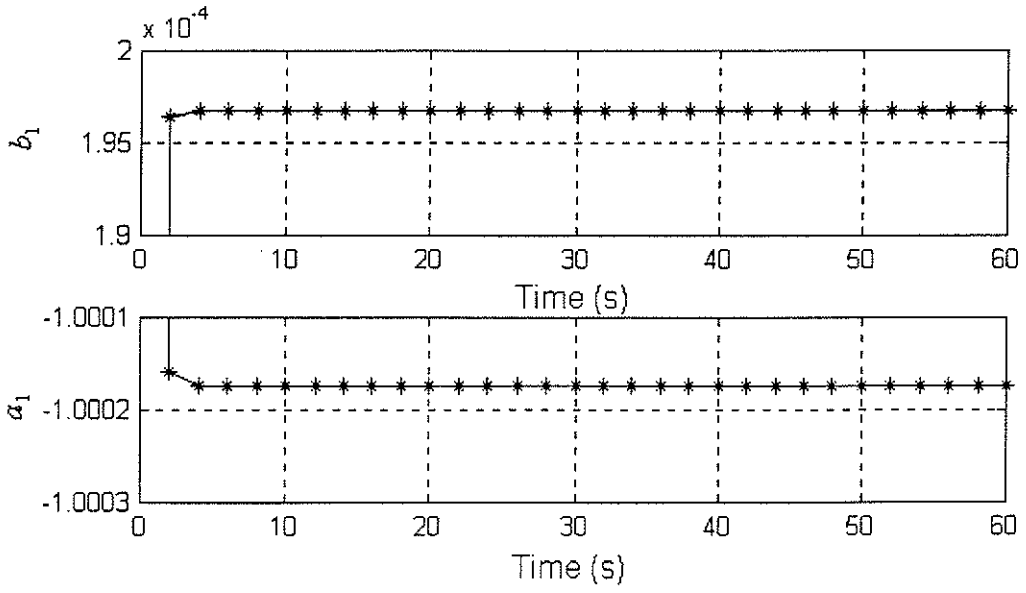

Fig. 5.19 ARX111 model coefficients using the batch LS method.

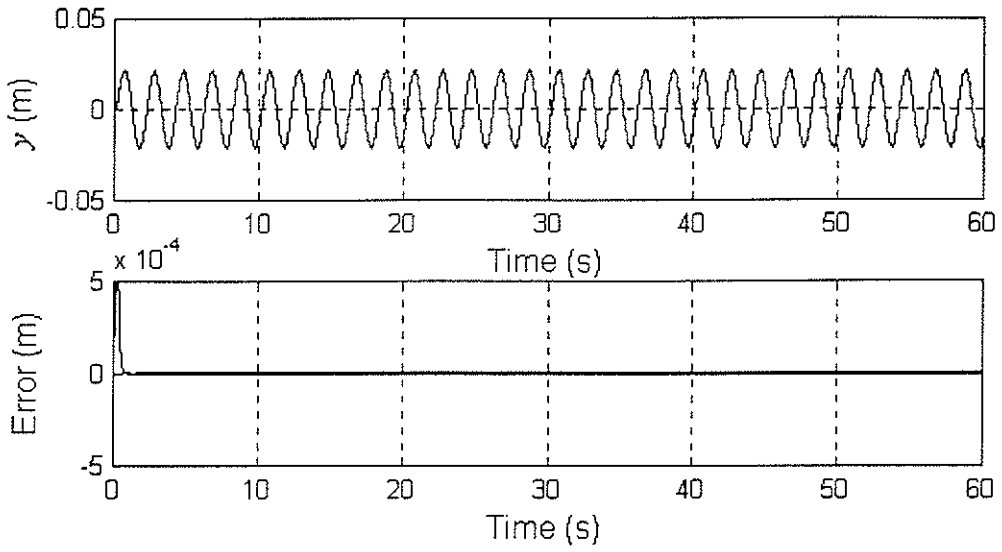

Fig. 5.20 ARX111 model output using the recursive LS method.

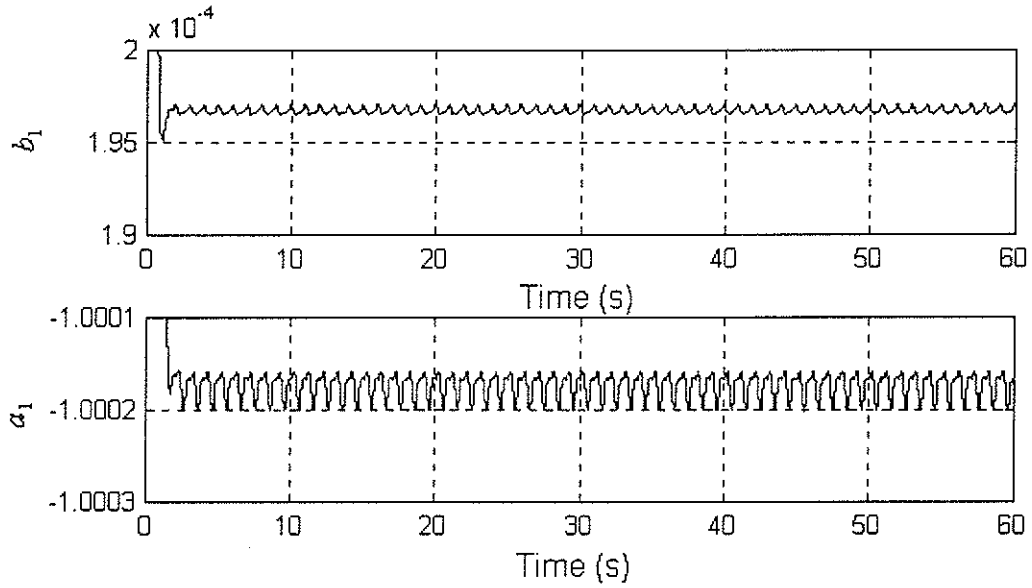

Fig. 5.21 ARX111 model coefficients using the recursive LS method.

The cost function value and the mean, maximum offset and variance of b_1 resulted from both the batch LS and the recursive LS methods are listed in Table 5.3. The cost function value resulted from the recursive LS method is 95.31% less than that resulted from the

batch LS method. The variance of b_1 resulted from the recursive LS method, however, is about 1.2269×10^{4} times larger than that resulted from the batch LS method

Table 5. 3 Batch LS versus Recursive LS for ARX111 model in the simulations.

	$J=\sum_{k=1}^{N}e^2(k)$	$\bar{b}_1=\frac{\sum_{k=1}^{N}b_{1k}}{N}$	$max(\lvert b_1-\bar{b}_1\rvert)$	$var(b_1)=\frac{\sum_{k=1}^{N}(b_{1k}-\bar{b}_1)^2}{N}$
Batch LS	9.1157×10^{-4}	1.9672×10^{-4}	4.1930×10^{-9}	2.2131×10^{-18}
Recursive LS	4.2770×10^{-5}	1.9672×10^{-4}	3.1607×10^{-7}	2.7153×10^{-14}

As stated in Section 4.1, for fault detection and isolation purposes, the variances of the estimated model coefficients affect the performance of the proposed FDI strategy. However, as compared to the recursive LS method, there are several shortcomings of the batch LS method:

1. Since the batch LS method has to buffer the past input and output data of the monitored system, it needs more storage space than the recursive LS method.
2. On-line fault detection is delayed because the batch LS method only produces a new set of estimated coefficients after it collects all the samples needed, while the recursive LS method can estimate a new set of coefficients once a new sample is received.

5.3 Fault Representation

For the hydraulic actuator, the exact value of the physical parameters listed in Table 5.1 may not be known and sometimes, the values of these parameters may change due to factors such as temperature and fault conditions. If the change in a parameter does

not affect the coefficients of the selected model that represents the system, this change is said to be undetectable. If several changes affect the coefficients of the model that represents the system in the same way, then they are said to be unidentifiable. The task of fault detection and isolation is to detect the fault condition and then to identify it.

As stated in Section 2.2.2, even for linear time-invariant (LTI) systems, the mapping function between the estimated model coefficients and the physical parameters, described by equation (2-16), cannot be always obtained. For the nonlinear hydraulic system in equation (4-16), the relationship between the coefficients of the ARX models and the physical parameters in Table 5.1 is indirect, which makes the task of fault detection and isolation for general cases very difficult. In order to show the concept of fault detection and isolation for nonlinear systems in feature space in this work, only faults originating from two specific sources, i.e., supply pump pressure, P_s, and equivalent viscous damping coefficient, d, are considered. The simulation study is, therefore, divided into three studies. In case I, fault conditions originating from only the supply pump pressure, P_s. In case II, fault conditions originating from only the equivalent viscous damping coefficient, d. In case III, a more complicated situation, fault conditions may originate from either the supply pump pressure or equivalent viscous damping coefficient.

5.3.1 FDI of Incorrect Supply Pump Pressure

Figure 5.22 shows coefficients of the ARX111 model for different supply pump pressures. It can be seen that for every $\pm 10\%$ change of supply pump pressure, the change of b_1 is approximately $\pm 5\%$. Although a_1 is also affected by the change in

supply pump pressure, when supply pump pressure changes by $\pm 50\%$, the change of a_1 is less than $\pm 0.01\%$. Therefore, b_1 can be used for fault detection and isolation of incorrect supply pump pressure. To exemplify this fault detection and isolation strategy, the following assumptions are made:

- Normal condition is defined as $900 \leq P_s \leq 1{,}100$ psi.
- Fault condition I is defined as $1{,}100 < P_s \leq 1{,}500$ psi
- Fault condition II is defined as $500 \leq P_s < 900$ psi

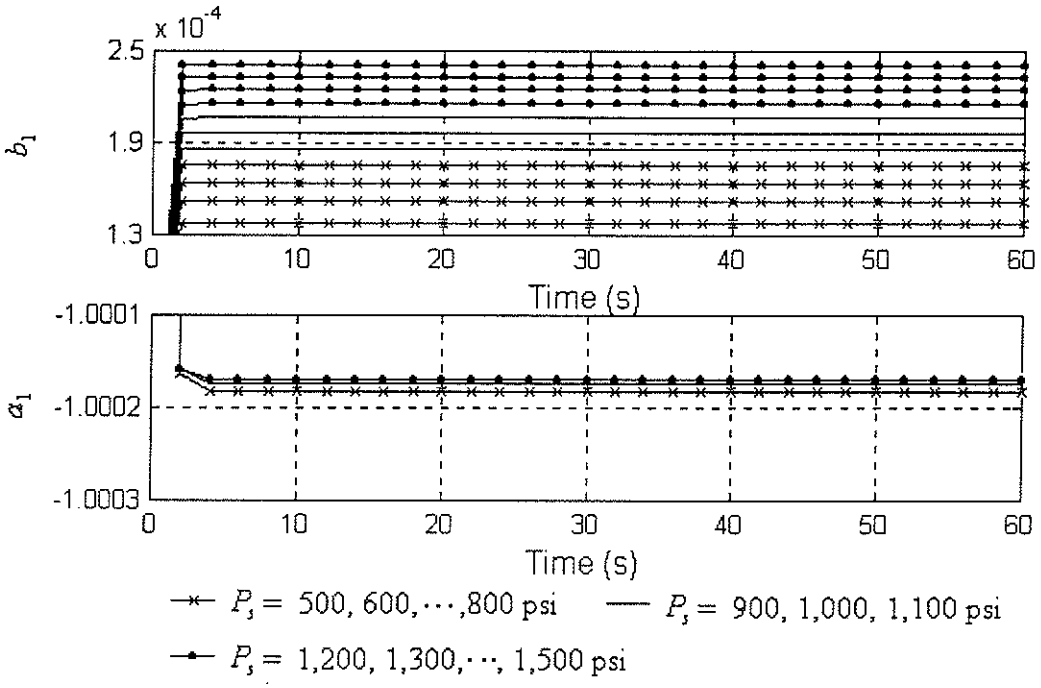

Fig. 5.22 Coefficients of ARX111 model for various supply pump pressures.

Based on the above assumptions, the fault detection and isolation logic for supply pump pressure failures is developed as below:

- If the estimated coefficient b_1 is larger than 2.10×10^{-4}, the monitoring system assumes that the system is working in fault condition I.

- If the estimated coefficient b_1 is in the range of $1.80\times10^{-4} \le b_1 \le 2.10\times10^{-4}$, the monitoring system assumes that the system is working under normal conditions.
- If the estimated coefficient b_1 is less than 1.80×10^{-4}, the monitoring system assumes that the system is working in fault condition II.

The performance of the proposed fault detection and isolation logic is tested in the following way. Initially, the system is run with the supply pump pressure, P_s, at 1,000 psi. After $t = 15$ sec, the supply pump pressure is increased to 1,250 psi. The supply pump pressure is brought down to the normal value of 1,000 psi at $t = 30$ sec. At $t = 45$ sec, the supply pump pressure is reduced to 750 psi. The control signal, u, system output, y, and estimated coefficients for this test are plotted in Figs. 5.23 and 5.24.

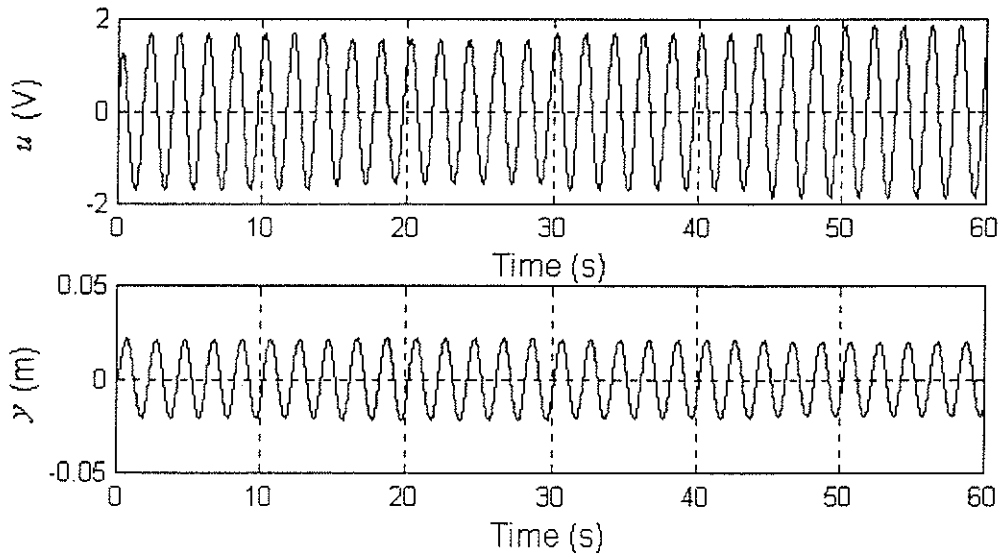

Fig. 5.23 Control signal and system output in FDI of incorrect supply pump pressure.

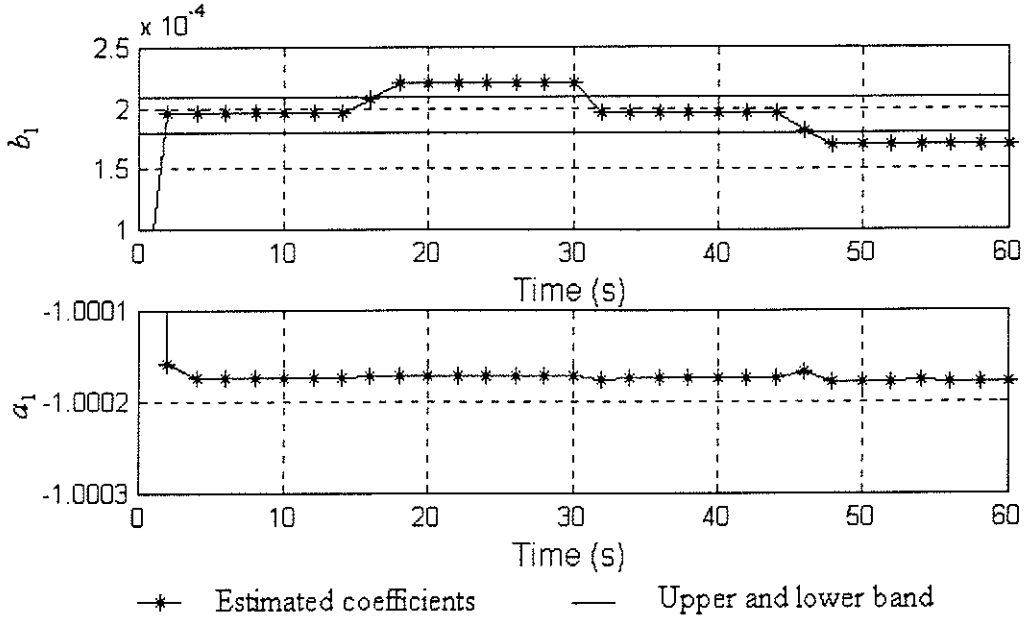

Fig. 5.24 FDI of incorrect supply pump pressure.

Figure 5.24 shows that at $t = 16$ sec, the value of b_1 begins to increase. The monitoring system triggers the alarm for fault condition I at $t = 18$ sec, when the value of b_1 is above the upper band. At $t = 32$ sec, the alarm for fault condition I is eliminated as the value of b_1 falls down to the normal range. At $t = 48$ sec, the alarm for fault condition II is triggered because the value of b_1 is below the lower band. By comparing with the actual working condition of the system, it is clear that the fault detection and isolation logic developed above not only detects the incorrect supply pump pressure, but also distinguishes between increased and decreased supply pump pressure faults. At the same time, this experimental test shows the delay for the fault detection. For example, the supply pump pressure is increased to 1,250 psi at $t = 15$ sec, but the monitoring system triggers the alarm at $t = 18$ sec. This delay is due to buffering action in the batch LS method as stated in section 5.2.

5.3.2 FDI for Changes in Equivalent Viscous Damping Coefficient

The coefficients of the ARX111 model according to different values of the equivalent viscous damping coefficient d are plotted in Fig. 5.25. Simulation results show that when d increases, the value of b_1 decreases. For every $\pm 10\%$ change of equivalent viscous damping coefficient, the value of a_1 changes less than $\pm 0.01\%$, however, the value of b_1 changes about $\pm 0.07\%$. Similarly to Section 5.3.1, the following assumptions are made:

- Normal condition is defined as $900 \leq d \leq 1{,}100$ N/(m/s).
- Fault condition *III* is defined as $1{,}100 < d \leq 1{,}500$ N/(m/s).
- Fault condition *IV* is defined as $500 \leq d < 900$ N/(m/s).

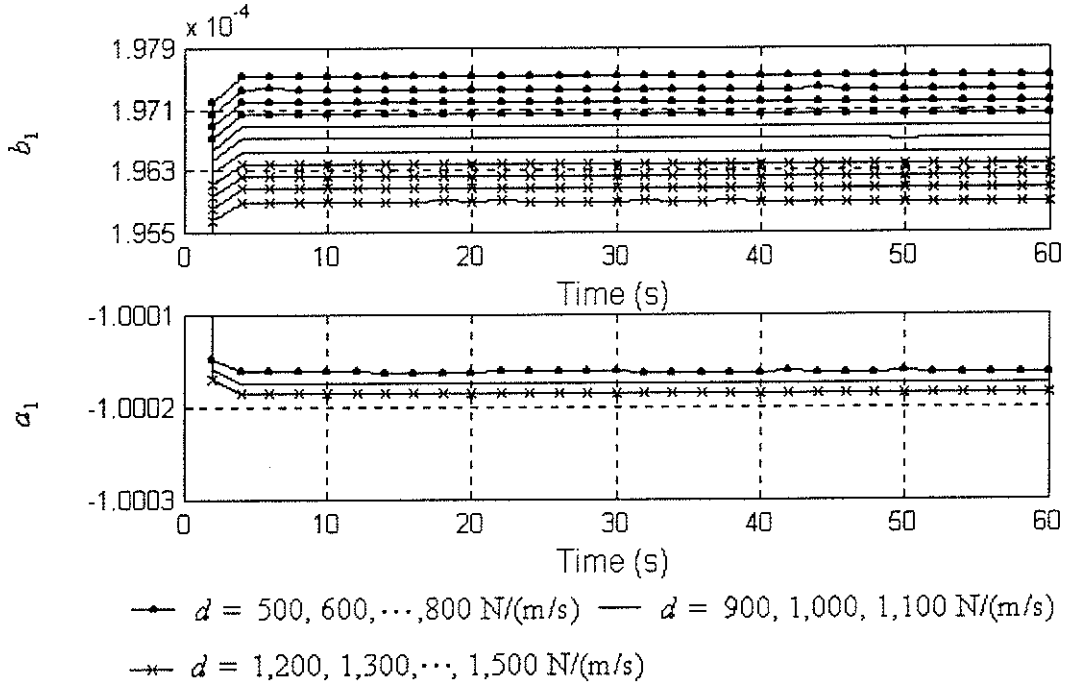

Fig. 5.25 Coefficients of ARX111 model for various equivalent viscous damping coefficients.

Since b_1 can reflect the change in equivalent viscous coefficient, d more precisely than a_1, as in Section 5.3.1, direct threshold checking for b_1 is selected as the fault detection and isolation logic, which is expressed as below:

- If the estimated coefficient b_1 is less than 1.9645×10^{-4}, the monitoring system assumes that the system is working in fault condition *III*.
- If the estimated coefficient b_1 is in the range of $1.9645\times10^{-4} \le b_1 \le 1.9695\times10^{-4}$, the monitoring system assumes that the system is working under normal conditions.
- If the estimated coefficient b_1 is lager than 1.9695×10^{-4}, the monitoring system assumes that the system is working in fault condition *IV*.

The performance of this fault detection and isolation logic is tested in the following way. At the beginning, the system is run with $d = 1{,}000$ N/(m/s). At $t = 15$ sec, the value of d is increased to 1,250 N/(m/s). The value of d is brought down to 1,000 N/(m/s) after $t = 30$ sec. At $t = 45$ sec, the value of d is reduced to 750 N/(m/s). The control signal, u, system output, y, and estimated coefficients for this test are plotted in Figs. 5.26 and 5.27.

Figure 5.27 shows that the monitoring system triggers the alarm for fault condition *III* at $t = 18$ sec when the value of b_1 is below the lower band. The alarm is eliminated at $t = 32$ sec when the value of b_1 returns to the normal range. At $t = 48$ sec, the alarm for fault condition *IV* is triggered because the value of b_1 is above the upper band. This shows that the fault detection and isolation logic developed above can successfully detect the fault condition originating from changes in the equivalent viscous

damping coefficient, d, and can also distinguish between fault conditions of increased and decreased equivalent viscous damping coefficient. The delay of the fault detection is due to the buffering action in the batch LS method as stated in Section 5.2.

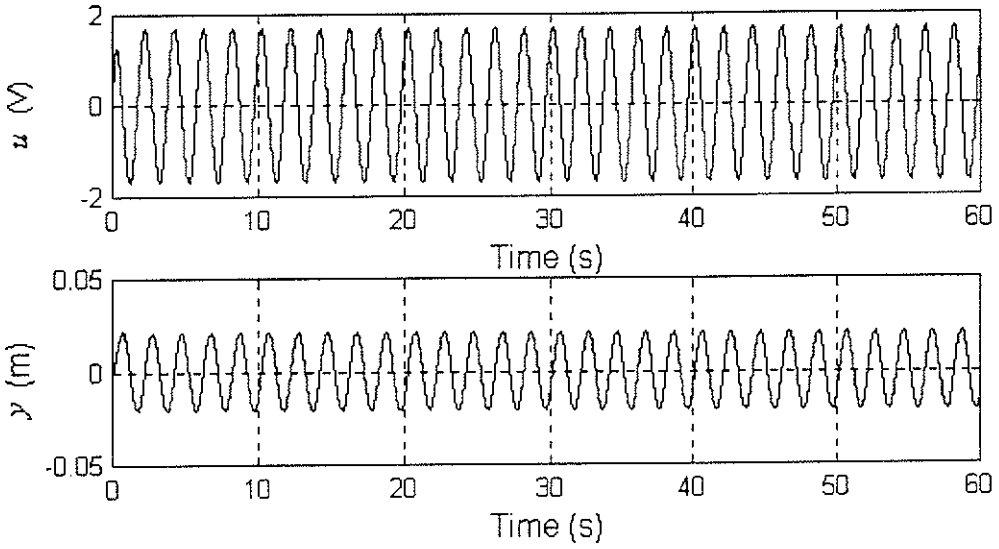

Fig. 5.26 Control signal and system output in FDI for changes in equivalent viscous damping coefficient.

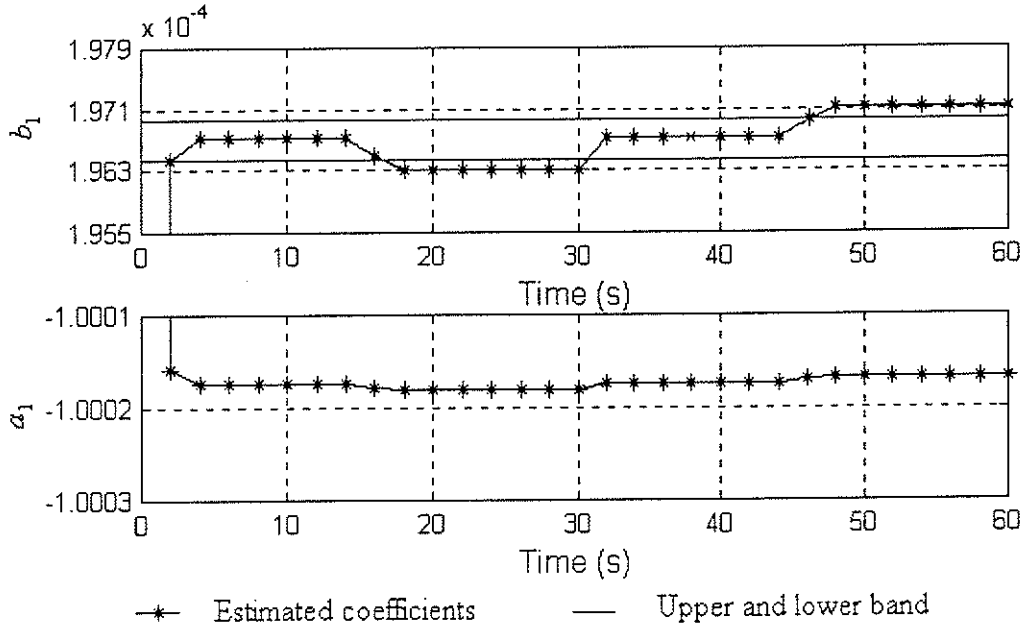

Fig. 5.27 Coefficients of ARX111 model in FDI for changes in equivalent viscous damping coefficient.

5.3.3 FDI for both Incorrect Supply Pump Pressure and Changes in Equivalent Viscous Damping Coefficient

The case where fault conditions originate either from incorrect supply pump pressure, P_s, or a change in the equivalent viscous damping coefficient, d, is studied. Since a_1 cannot reflect the change of the physical parameter in either case discussed in Sections 5.3.2 and 5.3.3, threshold checking on b_1 is the only choice left for developing fault detection and isolation logic in the constructed two dimensional feature space.

By comparing Fig 5.22 with Fig 5.25, it is seen that, the variation range of b_1 ($1.9550\times10^{-4} < b_1 < 1.9790\times10^{-4}$) due to the change of the equivalent viscous damping coefficient, d, is completely covered by the variation range of b_1 ($1.3000\times10^{-4} < b_1 < 2.5000\times10^{-4}$) due to the change in the supply pump pressure, P_s. Further study reveals that when the equivalent viscous damping coefficient, d, changes from 500 to 1,500 N/(m/s), the variation of b_1 still falls between the lower band ($b_1 = 1.8000\times10^{-4}$) and upper band ($b_1 = 2.1000\times10^{-4}$) chosen for detecting incorrect supply pump pressure, P_s. This implies that, as compared with faults originating from incorrect supply pump pressure, change of $\pm 50\%$ in the equivalent viscous damping coefficient, d, from its normal value is not detectable through direct threshold checking of estimated model coefficients.

This reveals the shortcoming of the strategy developed in Chapter 3. Since there is no direct one to one mapping from the estimated coefficients to the actual physical parameters, the following situations may occur:

- The change of different actual physical parameters may have the same effect on the estimated model coefficient.
- As compared to the effects of one physical parameter change, the effects of another may become undetectable.

These situations may lead to the normal and fault regions corresponding to different physical parameters overlapping with each other. This makes the task of fault detection and isolation more challenging.

Chapter 6 Experimental Results

Figure 6.1 shows the experimental test station. It consists of an electrohydraulic servovalve, a power supply unit, one main actuator, two slave actuators and a needle valve. The computer system used for control and monitoring purposes is a personal computer with a Pentium III CPU running under the Windows 98 operating system. The communication between the computer and the test station is performed by two I/O boards. The CIO-DAS16F board from Omega Engineering Inc. is used to convert digital control signals to analog control signals. A quadrature encoder board from Keithley measures the displacement of the hydraulic rod.

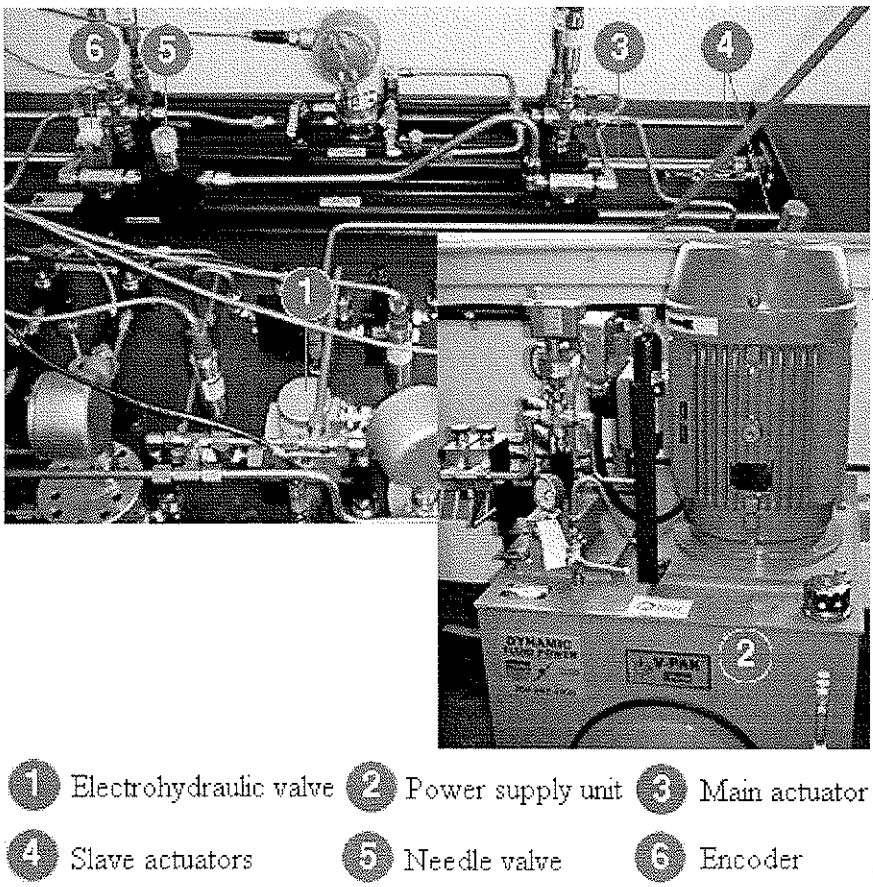

Fig. 6.1 Hydraulic actuator test station.

The power supply unit can provide fluid at different pressures. The normal working condition is defined when the power supply unit provides fluid at 2,000 psi and the two slave actuators are disconnected from the main one. First, an ARX model is selected to represent the behavior of the system under normal condition. Next, the fault detection and isolation capability of the chosen ARX model is studied for incorrect supply pump pressure and changes in equilvalent viscous damping coefficient.

6.1 Model selection

Under normal conditions, the actuator rod is tracking the reference position signal

$$r(n) = A\sin(2\pi\frac{f}{f_s}n) \tag{6-1}$$

under a proportional controller around the middle stroke. In equation (6-1), A is the amplitude of the rod displacement, f is the frequency of the reference signal, and f_s is the sampling frequency. In this experiment, $A = 0.0254$ m, $f = 0.5$ Hz, and $f_s = 200$ Hz. The typical reference signal, r, control signal, u, and rod displacement, y are shown in Figs. 6.2 to 6.4. Signals used for the monitoring system are the control signal, u and rod displacement signal, y.

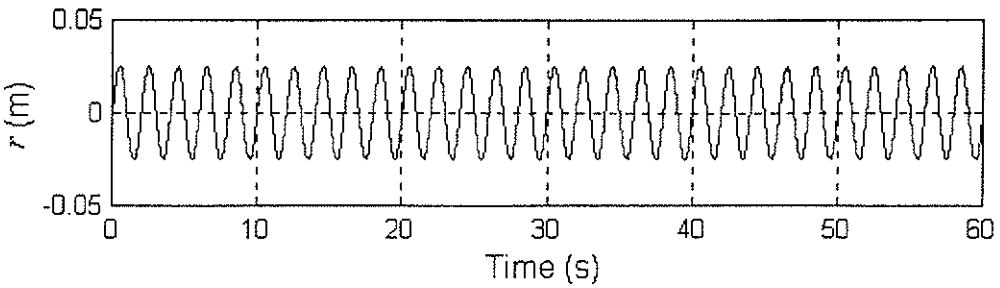

Fig. 6.2 Reference signal.

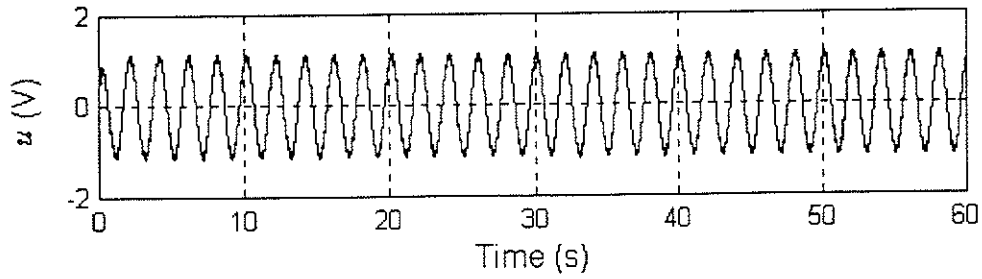

Fig. 6.3 Control signal.

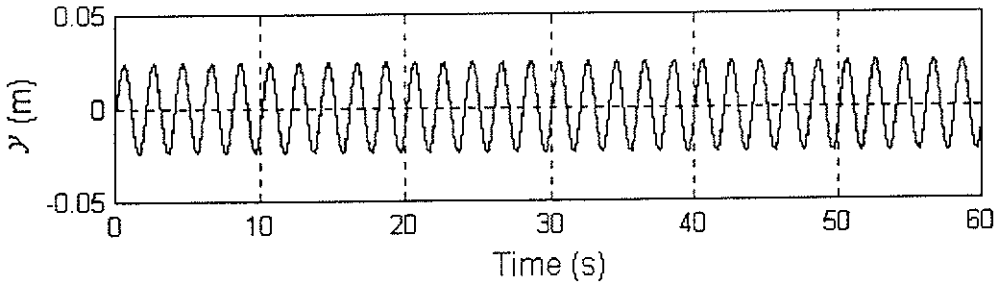

Fig. 6.4 Rod displacement.

The feature extraction is carried out by representing the input-output relationship of the monitored system by an ARX model. As in Chapter 5, the signals used for model selection purposes are one period of input and output data pairs (see Fig. 6.5).

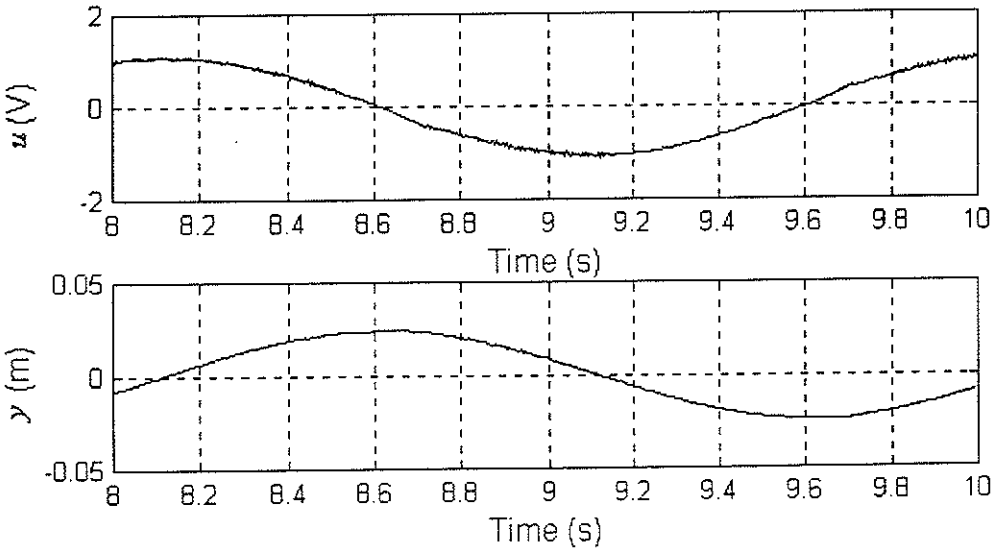

Fig. 6.5 Input and output data pairs for model selection.

In order to determine the structure i.e., the order of the ARX model, various structures are tried. The model coefficients are estimated by using the batch LS method described by equation (2-10). The corresponding error signal between the system and the model outputs is shown in Figs. 6.6 to 6.10.

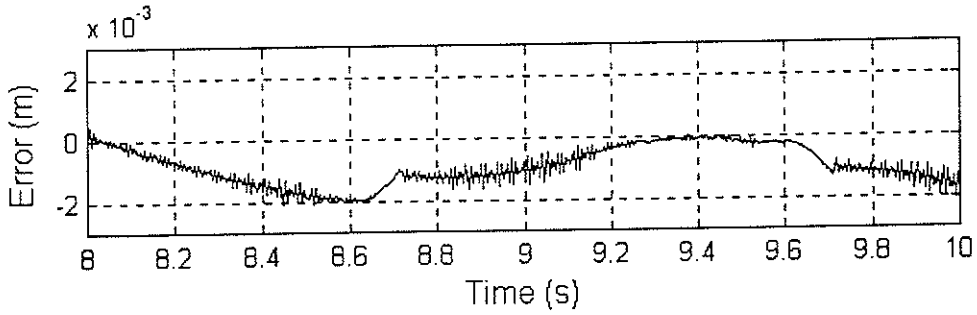

Fig. 6.6 Error signal corresponding to ARX111 model.

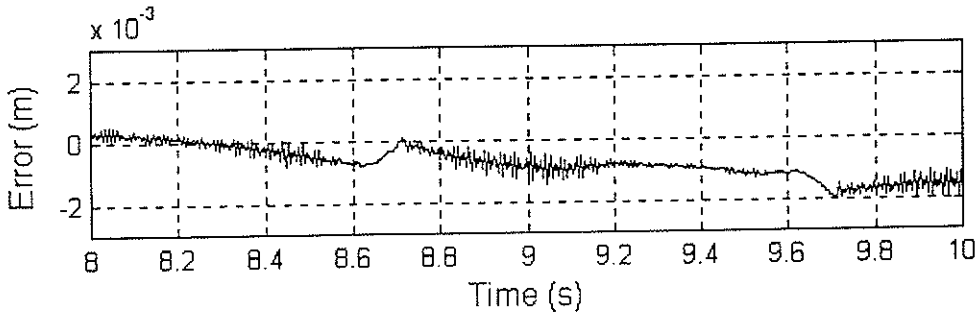

Fig. 6.7 Error signal corresponding to ARX211 model.

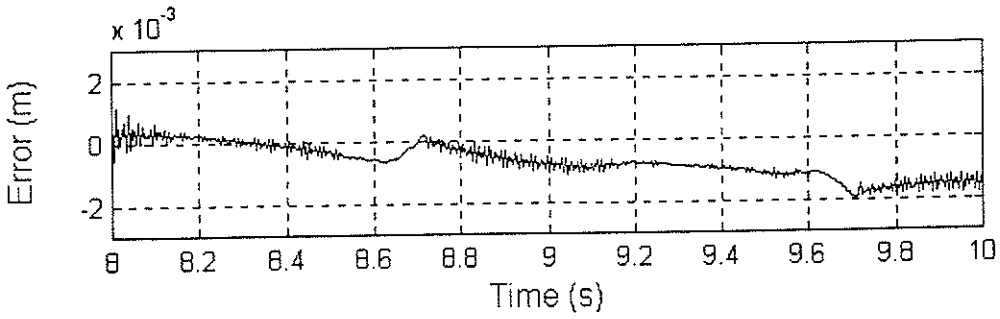

Fig. 6.8 Error signal corresponding to ARX311 model.

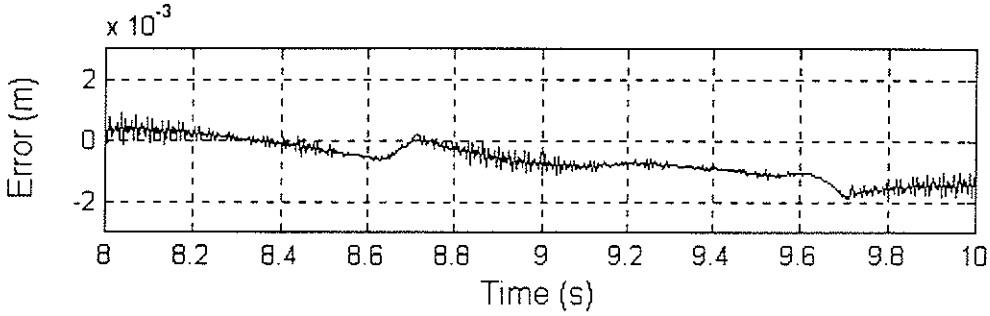

Fig. 6.9 Error signal corresponding to ARX411 model.

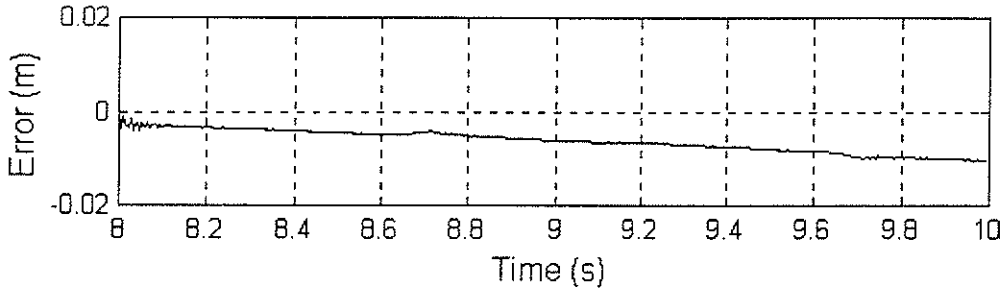

Fig. 6.10 Error signal corresponding to ARX421 model.

Further experiments showed that the ARX321, ARX331, ARX431 and ARX441 models estimated by the batch LS method cannot approximate the system output. Figures pertaining to these models are not shown. Values of the cost function, as described by equation (5-4), for ARX111, ARX211, ARX311, ARX411 and ARX421 models are presented in Table 6.1.

Table 6.1 Cost function values for different models.

Model	$E(m^2)$
ARX111	4.8595×10^{-4}
ARX211	3.7411×10^{-4}
ARX311	3.5075×10^{-4}
ARX411	3.1446×10^{-4}
ARX421	1.7748×10^{-2}

Table 6.1 indicates that ARX411 model has the minimum cost function value. It also shows that increasing the value of n will further reduce the value of the cost function. For example, when ARX911 is used, the value of the cost function is 2.59156×10^{-4}. However, as was stated in Chapter 5, a higher order model may not be a good choice from the viewpoint of fault detection and isolation. Another issue to be considered is the variances of the estimated model coefficients. Since variances of the estimated model coefficients reflect the distribution of the points representing the system in the feature space, a large variance is not good for fault detection and isolation. Using the batch LS algorithm, the estimated coefficients of ARX211 and ARX411 and corresponding error signals between the system and model outputs are presented in Figs. 6.11 and 6.12. It is seen that the estimated coefficients of ARX411 have a larger variance than those of ARX211 model. Taking both the value of cost function and variance of the estimated model coefficients into consideration, ARX211 is selected as the best fit model structure.

Figure 6.13 shows the estimated ARX211 coefficients using the recursive LS method and the corresponding error signal. The cost function value and the mean, maximum offset and variance of b_1 are outlined in Table 6.2.

Table 6. 2 Batch LS versus Recursive LS for ARX211 model in the experiments.

	$J=\sum_{k=1}^{N}e^2(k)$	$\bar{b}_1=\frac{\sum_{k=1}^{N}b_{1k}}{N}$	$max(\lvert b_1-\bar{b}_1\rvert)$	$var(b_1)=\frac{\sum_{k=1}^{N}(b_{1k}-\bar{b}_1)^2}{N}$
Batch LS	0.0090	6.5229×10^{-4}	4.4956×10^{-6}	2.2573×10^{-12}
Recursive LS	3.9927×10^{-4}	6.4924×10^{-4}	5.7642×10^{-5}	2.1453×10^{-10}

It is seen that the cost function value resulted from the recursive LS method was 95.56% less than that resulted from the batch LS method. The variance of b_1 resulted from the recursive LS method was about 95 times larger than that resulted from the batch LS method. Since large variance is not desirable for fault detection and isolation, the batch LS method is employed in this study.

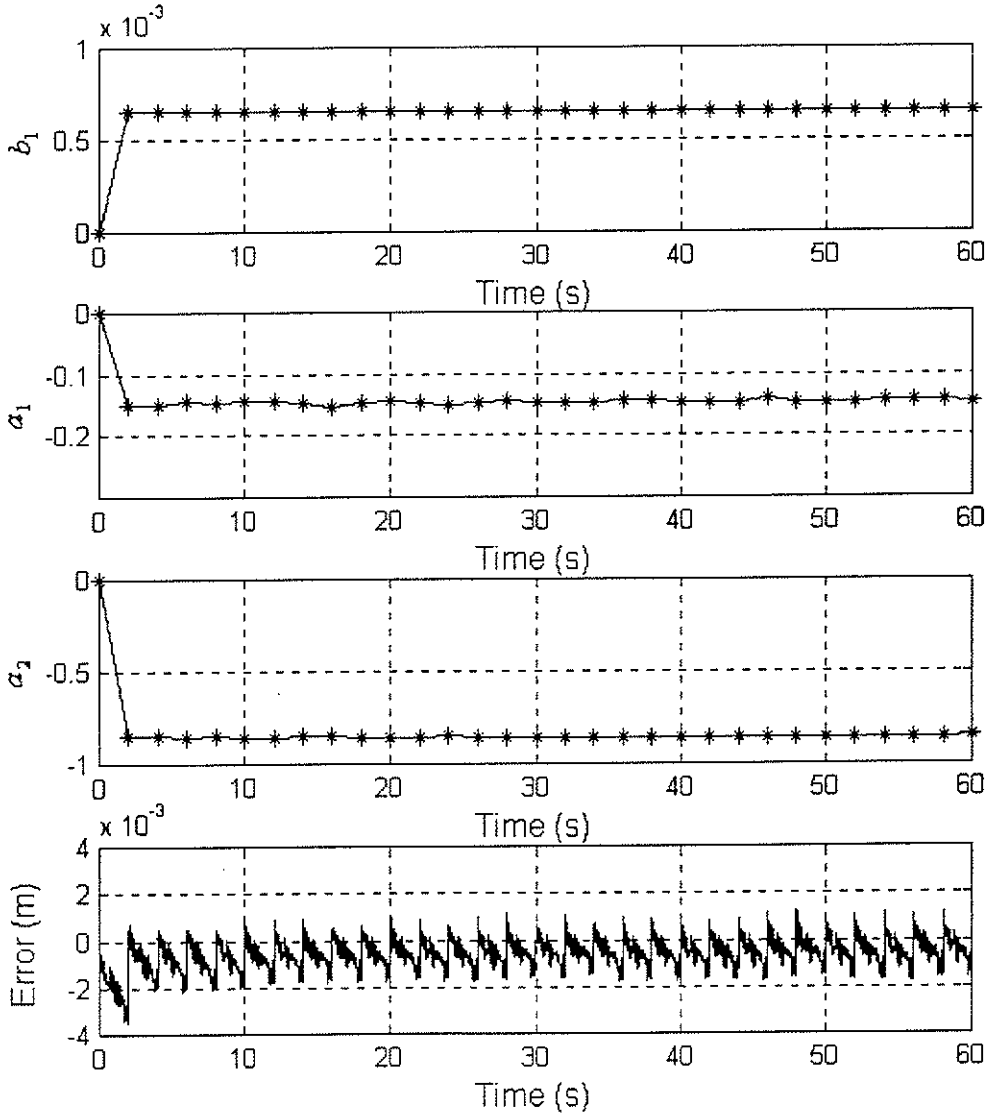

Fig. 6.11 Coefficients and error signal of ARX211 model using the batch LS method.

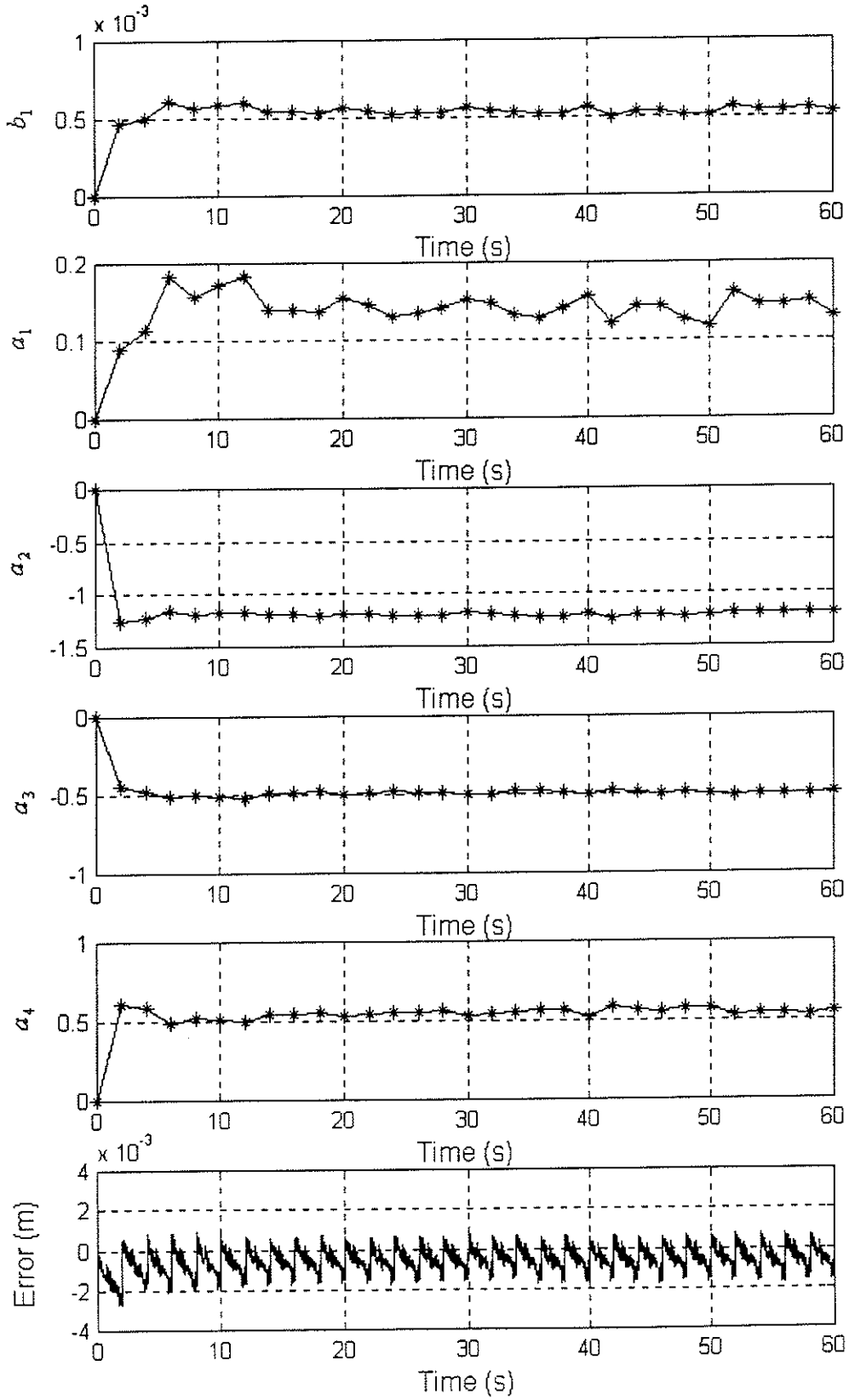

Fig. 6.12 Coefficients and error signal of ARX411 model using the batch LS method.

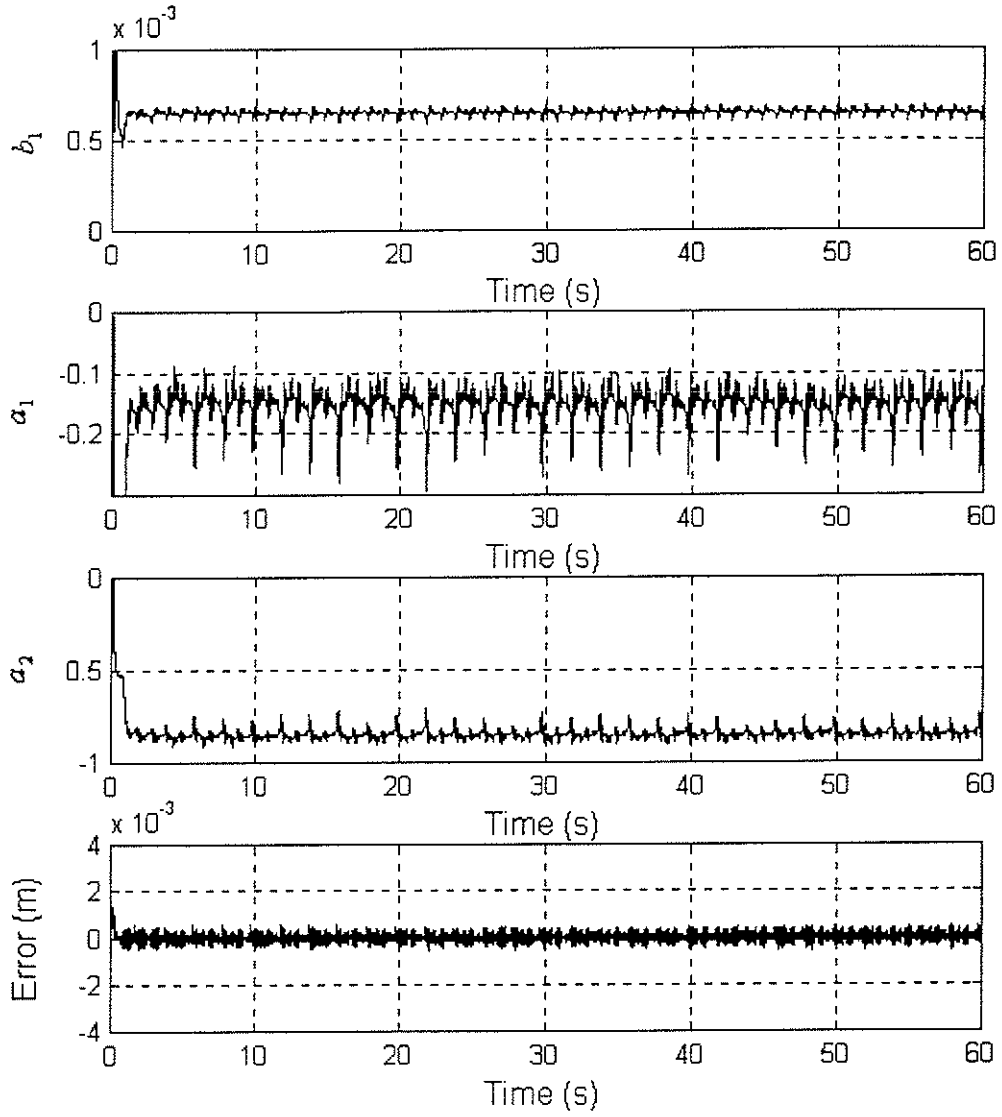

Fig. 6.13 Coefficients and error signal of ARX211 model using the recursive LS method.

6.2 Fault Detection and Isolation

By selecting the ARX211 model to describe the behavior of the system is presented by the parameter vector $\theta^T = (b_1, a_1, a_2)$. The batch LS method is used for estimating values of b_1, a_1, and a_2. In this section, fault diagnosis for incorrect supply pump pressure and changes in equivalent viscous damping coefficient is presented.

6.2.1 FDI of Incorrect Supply Pump Pressure

In the following experiments, the system was run with a supply pump pressure, P_s, of 1,500 psi, 1700 psi, 2,000 psi, 2,300 psi and 2,500 psi. With the batch LS method, the estimated coefficients for the ARX211 model are shown in Fig 6.14.

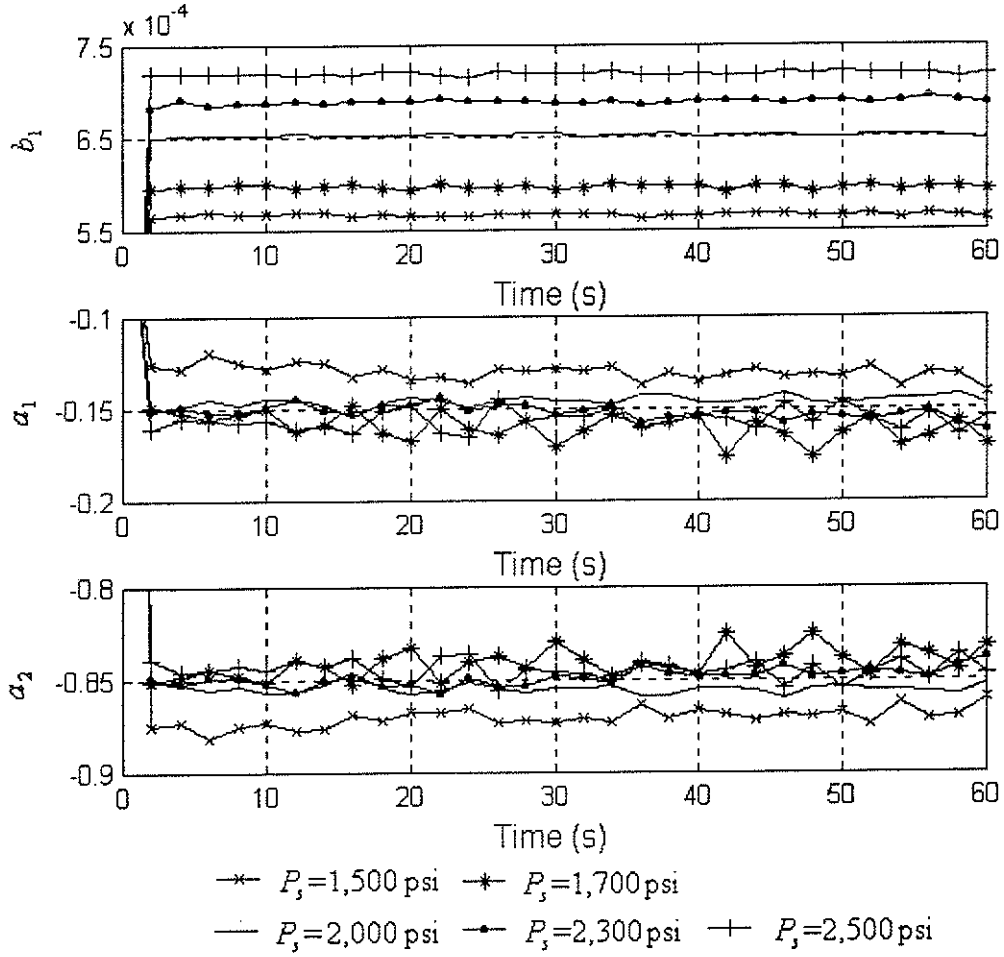

Fig. 6.14 Coefficients of ARX211 model for various supply pump pressures.

Figure 6.14 shows that b_1 changes proportionally with a change in the supply pump pressure. For every $\pm 10\%$ change in supply pump pressure, the value of b_1 changes by about $\pm 5\%$ Although a_1 and a_2 are also affected, the relationship between the change of supply pump pressure and the changes of a_1 and a_2 is not as obvious as in

the case of b_1. Therefore, threshold checking on b_1 is used to detect and potentially isolate the faults of incorrect supply pump pressure.

Fault detection and isolation logic below is developed for the following experimental test.

- If $b_1 > 6.700 \times 10^{-4}$, the monitoring system detects that the system is working under the condition that the supply pump pressure is increased.
- If $b_1 < 6.400 \times 10^{-4}$, the monitoring system detects that the system is working under the condition that the supply pump pressure is decreased.

In the experimental test, the system initially runs under normal conditions of P_s=2,000 psi. At $t \approx 13$ sec, the supply pump pressure is increased to 2,500 psi and, at $t \approx 28$ sec, the supply pump pressure is reduced to 1,500 psi. The estimated coefficients and upper and lower bands for b_1 are shown in Fig. 6.15. It is seen that at $t = 16$ sec, the value of b_1 is above the upper band and the monitoring system triggers the fault alarm for increased supply pump pressure. At $t = 30$ sec, the fault alarm for decreased supply pump pressure is triggered when the value of b_1 is below the lower band. This shows that threshold checking on b_1 can be employed as a fault detect and isolation strategy for incorrect supply pump pressure. The fault detection and isolation logic developed above can not only detect the fault conditions, P_s=1,500 and 2,500 psi, but also can isolate these two fault conditions.

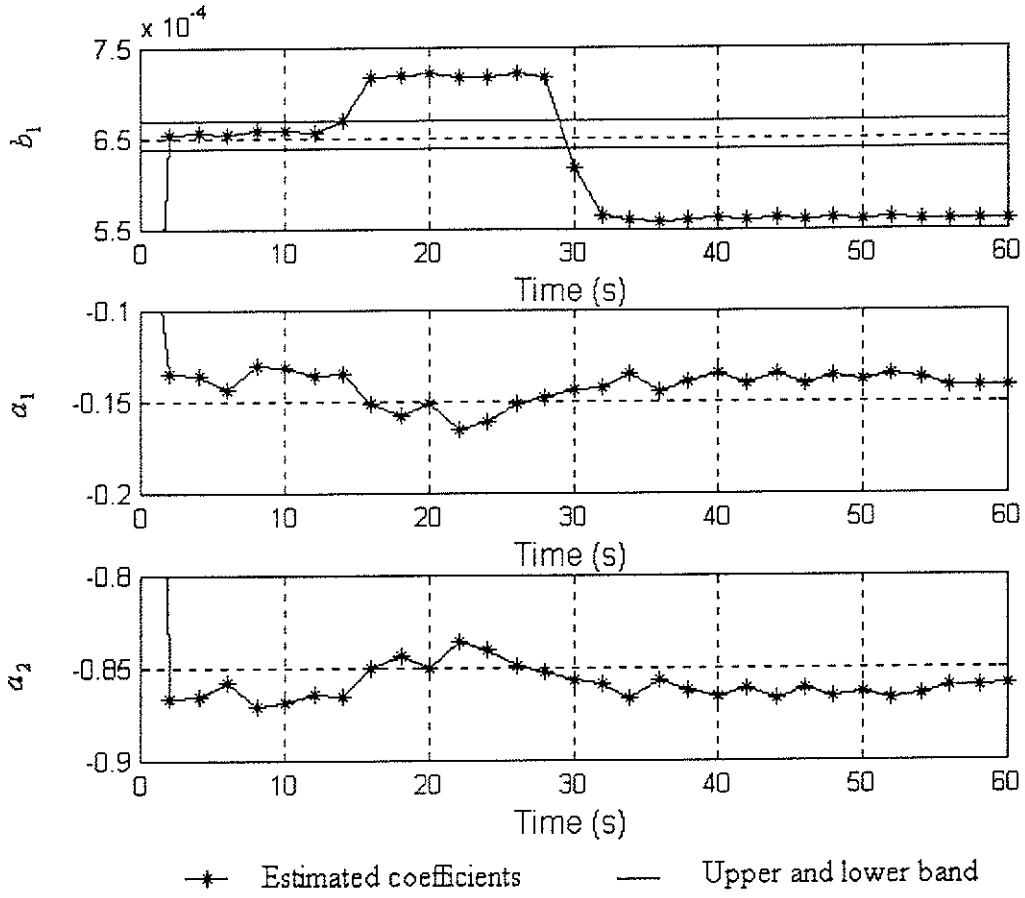

Fig. 6.15 FDI of incorrect supply pump pressure.

6.2.2 FDI for Changes in Equivalent Viscous Damping Coefficient

In order to simulate the changes in equivalent viscous damping coefficient, two slave actuators are connected to the main one, which changes physical parameters such as inertia and the equivalent viscous damping coefficient. This kind of fault condition cannot be detected by the traditional hardware redundancy based fault detection and isolation strategy.

In Fig. 6.16, the coefficients of the ARX211 model for the normal condition and the condition in which two slave actuators are connected to the main one and the needle valve is fully opened are presented.

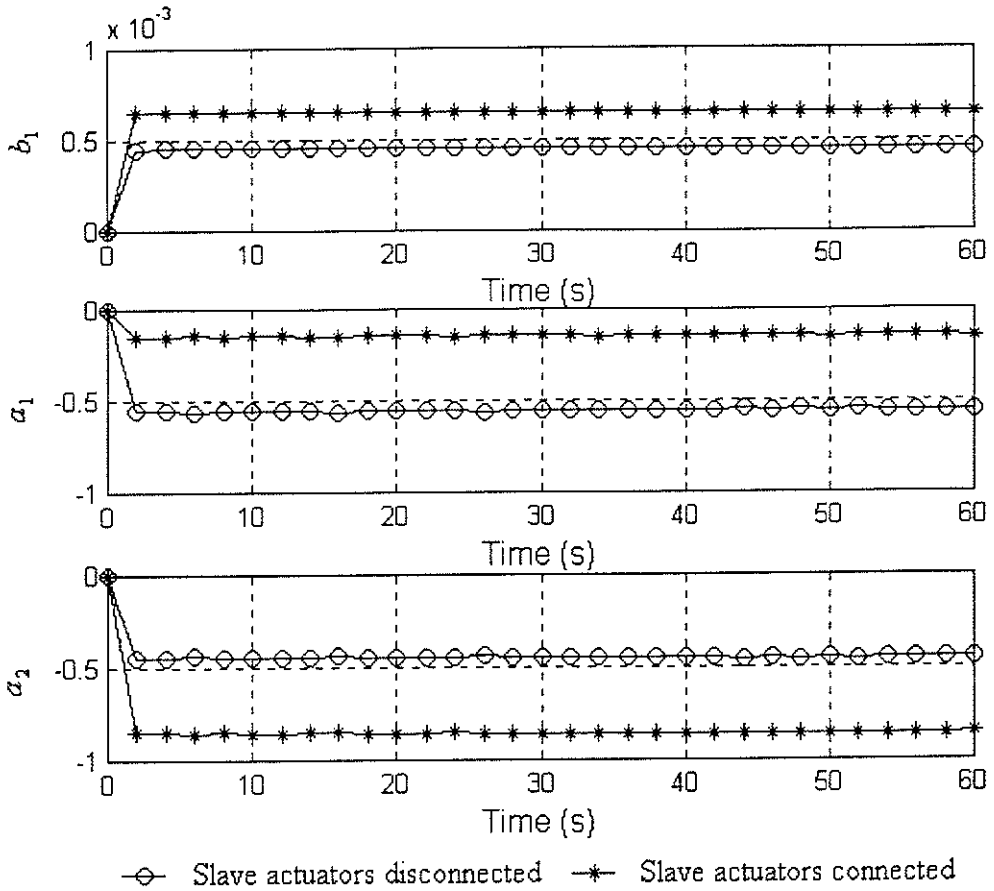

Fig. 6.16 Coefficients of ARX211 model with effects from two slave actuators.

Figure 6.16 clearly shows that by selecting a proper threshold value, direct threshold checking of b_1, a_1 or a_2 can easily separate these two conditions. Since in the lab environment, these two conditions cannot be switched when the system is running, an on-line fault detection experimental test, as was done for incorrect supply pump pressure, is not performed here.

By adjusting the needle valve with two slave actuators connected, the equivalent viscous damping coefficient, d, can be further changed. The estimated coefficients of the ARX211 for the fully open and 80% closed needle valve are presented in Fig. 6.17.

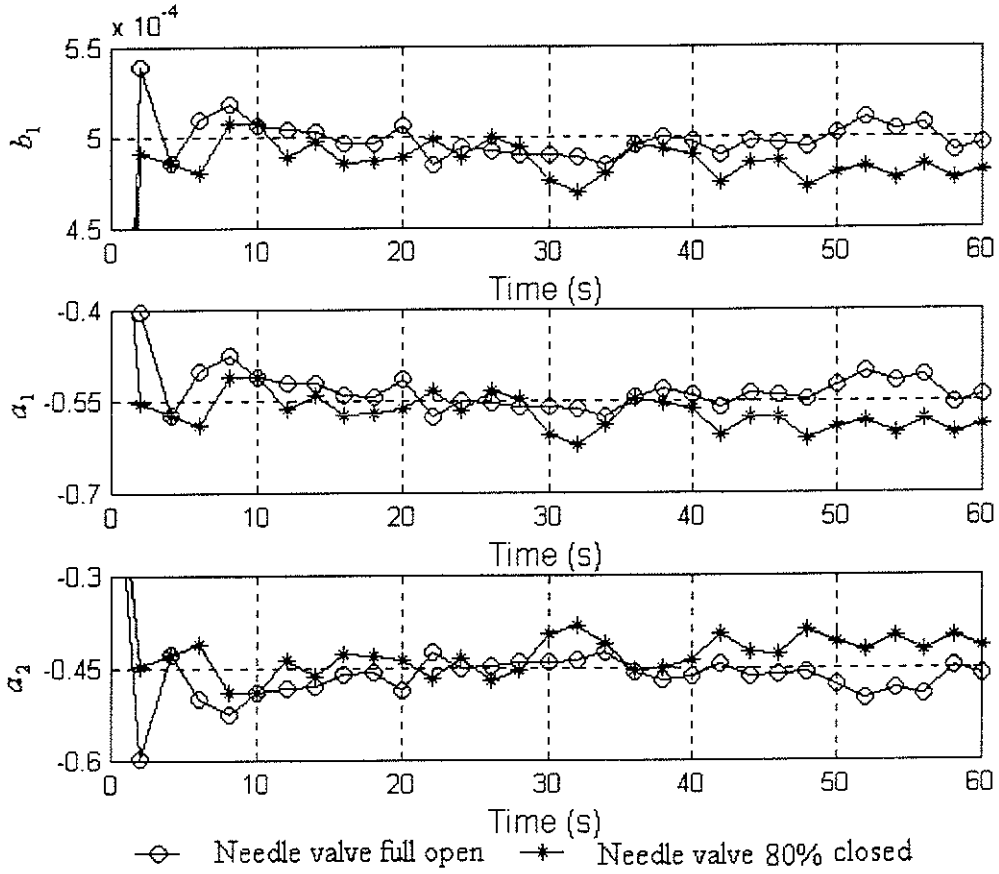

Fig. 6.17 Coefficients of ARX211 model with effects from the needle valve.

In Fig. 6.17, it is seen that the large variances of b_1, a_1 and a_2 make it impossible to separate these two conditions by direct threshold checking. This occurs because when the two slave actuators are connected, the structure of the system is changed and the ARX211 model selected for normal conditions (where two slave actuators are disconnected) is no longer a suitable model, and thus it cannot be employed to distinguish any further changes in equivalent viscous damping coefficient by direct threshold checking logic. This also shows the importance of selecting a proper model for the fault detection and isolation strategy discussed in this work. For such a case, different models other than ARX211 may be tried.

Chapter 7 Conclusions

In this thesis, a parameter estimation based fault detection and isolation strategy was employed for fault diagnosis of the supply pump pressure and equivalent viscous damping coefficient changes in a hydraulic servo-positioning system. A case where the hydraulic actuator tracks a sinusoid reference signal under a proportional controller was considered. The control signal and the resulting output position signal of the system were used to arrive at an appropriate auto-regressive with exogenous input (ARX) model to represent the relationship between the input and output signals. The ARX model structure was selected due to the real-time requirement of the monitoring system and the availability of powerful on-line model coefficient estimation methods, such as the least squares (LS) method. Direct threshold checking on the estimates of the model coefficients was then employed as the fault detection and isolation logic.

Both simulation and experimental results showed that a higher order ARX model could approximate the system dynamics more accurately than a lower order one. But the lower model could achieve higher resolution of fault detection. In the simulations, by selecting an ARX111 model, $\pm 10\%$ change in the supply pump pressure was clearly detected. Compared with the ARX111 model, the cost function value for the ARX411 model was 51.43% less, but the $\pm 10\%$ change in the supply pump pressure could not be clearly separated. Thus, the ARX111 model was chosen in the simulations. In the experimental tests, ARX211 was selected since it had a 23.01% lower cost function value than the ARX111 model. At the same time it showed small variances of the estimated coefficients.

Both simulation and experimental results showed that the models based on the recursive LS method could approximate the system output better than the ones derived by the batch LS method. However, the model coefficients resulting from the recursive LS method had larger variances than those obtained by the batch LS method. In the simulations, for the ARX111 model, the cost function value resulting from the recursive LS method was 95.31% less than that resulting from the batch LS method. The variance of b_1 resulting from the recursive LS method, however, was about 1.2269×10^{4} times larger than that resulting from the batch LS method. In the experiments, for the ARX211 model, the cost function value resulting from the recursive LS method was 95.56% less than that resulting from the batch LS method. The variance of b_1 resulting from the recursive LS method was about 95 times larger than that resulting from the batch LS method. Based on these observations and the fact that large variances in the model coefficients would reduce the resolution of the fault detection strategy, the batch LS method was adopted in this thesis. The use of the batch LS method, however, led to a delay of about 3 seconds in the fault detection due to its buffering action in both simulation and experimental tests.

In the simulations, $\pm 10\%$ changes in the supply pump pressure and $\pm 10\%$ changes in the equivalent viscous damping coefficient from their normal values were detected by the proposed strategy. The proposed strategy, however, failed to achieve complete fault detection and isolation when the fault could originate from more than one physical parameter. Experiments also showed that the proposed strategy could achieve the detection of $\pm 10\%$ change of the supply pump pressure. But the change in the viscous damping coefficient could not be detected.

In future works, the proposed strategy can be extended in the following directions:

- Investigation of the nature of the faults that occur in the system in real applications and integrating field experience into the monitoring system.
- Development of more powerful fault detection and isolation logic than direct threshold checking on the estimated coefficients. Neural Networks, Sequence Analysis and other statistical pattern recognition methods should be applied.
- More general cases than the specific one considered in this work (tracking a specific reference signal) should be tried.
- Fault detection and isolation abilities for other physical parameter changes should be investigated.

References

[1] D.G. Luenberger, "Observing the State of a Linear System", *IEEE Transactions on Military Electronics*, Vol. MIL-8, pp. 74-80, April 1964.

[2] D.G. Luenberger, "Observers for Multivariable Systems", *IEEE Transactions on Automatic Control*, Vol. AC-11, No.2, pp. 190-197, April 1966.

[3] R.N. Clark, P.M. Frank and R.J. Patton, "Chapter 1: Introduction" in "Fault Diagnosis in Dynamic Systems Theory and Applications, (R.J. Patton, P.M. Frank and R.N. Clark, eds.)", Prentice Hall, Hertfordshire, UK, 1989.

[4] P.M. Frank and J. Wunnenberg, "Chapter 3: Robust Fault Diagnosis using Unknown Input Observer" in "Fault Diagnosis in Dynamic Systems Theory and Applications, (R.J. Patton, P.M. Frank and R.N. Clark, eds.)", Prentice Hall, Hertfordshire, UK, 1989.

[5] R. Isermann, "Chapter 7: Process Fault Diagnosis Based on Dynamic Models and Parameter Estimation Methods" in "Fault Diagnosis in Dynamic Systems Theory and Applications, (R.J. Patton, P.M. Frank and R.N. Clark, eds.)", Prentice Hall, Hertfordshire, UK, 1989.

[6] P. Van Dooren and P. Dewilde, "The Eigenstructure of an Arbitrary Polynomial Matrix", *Linear Algebra and Applications,* Vol. 50, pp. 545-579, 1983.

[7] P. Van Dooren, "The Computation of Kronecker's Canonical Form of a Singular Pencil", *Linear Algebra and Applications*, Vol. 27, pp. 103-140, 1979.

[8] H.E. Merritt, "Hydraulic Control Systems", John Wiley & Sons, NJ, 1967.

[9] L. Ljung and T. Söderström, "Theory and Practice of Recursive Identification", MIT Press, London, England, 1983.

[10] K. Ogata, "Modern Control Engineering", 2nd ed., Prentice Hall, NJ, 1990.

[11] W.J. Thayer, "Transfer Functions for Moog Servovalves", *Technical Bulletin 103*, Moog, Inc., NJ, 1967.

[12] C.M. Bishop, "Neural Networks for Pattern Recognition", Oxford University Press, NJ, 1995.

[13] H. Tan and N. Sepehri, "Parametric Fault Diagnosis for Electrohydraulic Cylinder Drive Units", *IEEE Transactions on Industrial Electronics*, Vol. 49, pp. 96-106, Feb. 2002.

[14] D. Yu, D.N. Shields and S. Daley, "A bilinear fault detection observer and its application to a hydraulic drive system", *Int. J. Control*, Vol. 64, No. 6, pp. 1023-1047, 1996.

[15] G.J. Preston, D.N. Shields and S. Daley, "Application of a robust nonlinear fault detection observer to a hydraulic system", *Proc. UKACC Int. Conf. on Control'96*, Exeter, UK, pp.1484-1489, Sept. 1996.